Received: 25 October 2024 | Revised: 8 January 2025 | Accepted: 2 February 2025

DOI: 10.1111/ijac.15087

International Journal of Applied Ceramic Technology

REVIEW ARTICLE

Additive manufacturing of ceramics via the laser powder bed fusion process

Abid Ullah[1,2] | **Mussadiq Shah**[3] | **Zulfiqar Ali**[4] | **Karim Asami**[1] | **Asif Ur Rehman**[5] | **Claus Emmelmann**[1]

[1]Institute of Laser and Systems Technology, Hamburg University of Technology, Hamburg, Germany

[2]Centre for Additive Manufacturing, School of Engineering, RMIT University, Melbourne, VIC, Australia

[3]Institute of Chemical Technologies and Analytics, Technische Universität Wien, Vienna, Austria

[4]Department of Mechanical Engineering, The University of Hong Kong, Hong Kong, SAR, China

[5]Bartlett School of Sustainable Construction, University College London, London, UK

Correspondence
Abid Ullah, Institute of Laser and Systems Technology, Hamburg University of Technology, Hamburg D-21079, Germany.
Email: abid.ullah@tuhh.de

Mussadiq Shah, Institute of Chemical Technologies and Analytics, Technische Universität Wien, Vienna 1040, Austria.
Email: mussadiq.shah@tuwien.ac.at

Funding information
German Academic Exchange Service (DAAD); European Union's Horizon 2020 Research and Innovation Program under the Marie Skłodowska-Curie Grant Agreement, Grant/Award Number: 101034328

Abstract

Additive manufacturing (AM) of ceramics presents both exciting opportunities and significant challenges, particularly with the laser-based AM processes. Ceramics are known for their special properties, such as high strength, corrosion resistance, and temperature stability, but their inherent brittleness and high processing demands make AM more complex. This review provides an updated overview of the most common AM techniques for ceramics, including direct energy deposition, binder jetting, laminated object manufacturing, and material extrusion-based techniques. However, the focus is placed on the laser powder bed fusion (LPBF) of ceramics, a technique that has gained increasing attention for its ability to fabricate complex ceramic parts with enhanced quality. The review delves into the key causes of critical defects commonly observed in LPBF, such as porosity, cracking, spattering, and surface roughness. Recent advancements in addressing these issues are discussed, along with the limitations of current defect prevention strategies. Furthermore, the review provides an updated analysis of the mechanical properties of LPBF-fabricated ceramics, giving insights into how processing parameters influence the performance of ceramic LPBF-printed parts. Modeling and simulation techniques are also reviewed, highlighting their role in enhancing understanding of ceramic behavior during LPBF. Overall, this review highlights recent progress and current challenges in ceramic AM techniques, while exploring future research opportunities, such as process optimization and defect prevention strategies.

KEYWORDS
additive manufacturing, ceramics, defects, laser powder bed fusion, modeling and simulation, properties

1 | INTRODUCTION

Ceramics are heat-resistant, inorganic, and nonmetallic materials. They are broadly categorized into two groups based on their applications: conventional ceramics and advanced ceramics.[1,2] Traditionally, the term "*ceramic*" refers to clay-based products such as pottery, bricks, tableware, tiles, and so on. Advanced ceramics are the most vital ceramics that differ from ordinary ceramics in various chemical and mechanical properties, including tensile strength, fracture toughness, wear resistance, and dielectric behavior.[1,3] Globally, advanced ceramics are known in various terms, including technical ceramics, high-performance ceramics, and high-tech ceramics, with terminology varying by region. Advanced structural ceramics, including materials like alumina, zirconia, silicon carbide, and titania, exhibit exceptional characteristics such as high mechanical strength, hardness, excellent resistance to wear and corrosion, and low thermal conductivity, making them suitable for a wide range of applications.[1,3–5] Furthermore, certain ceramics have good biocompatibility, allowing them to be used in biomedical applications such as dental and body prosthetics, as well as tissue engineering[3,6].

In worldwide industries, processing time and resource efficiency are crucial for manufacturing. As customer demands grow, product diversity and complexity increase, requiring advanced tools and techniques for optimal resource utilization. Ceramics production, both traditional and advanced, typically involves five steps: raw material acquisition, powder preparation, shaping, sintering, and finishing.[7] Complex ceramic parts are produced through conventional methods such as hot isostatic pressing (HIP), extrusion, injection molding, and casting,[8] which are in fact time-consuming and require costly equipment like drills, mills, and grinders.[9,10] Traditional fabrication techniques must be updated and developed further to meet modern demands for complex ceramic components, as they still face challenges in producing parts involving complex designs. High-strength oxide ceramics, known for their mechanical strength, wear resistance, and thermal stability, are ideal for high-end engineering applications.[11,12] Traditional methods often experience drawbacks, such as tool wear and sintering shrinkage, and typically require postprocessing for complete densification.[13–15] Due to the limitations of traditional manufacturing methods, such as lengthy processing times, high costs for complex designs, and challenges like tool wear and shrinkage, additive manufacturing (AM) offers a promising alternative by enabling the efficient production of intricate, high-performance ceramic components with greater design flexibility and reduced need for postprocessing.

AM is widely recognized as a pivotal development in modern fabrication, fundamentally changing design and production processes. Laser-based powder bed fusion (LPBF), also referred to as selective laser melting (SLM), has become a cornerstone of AM, renowned for its superior geometric accuracy. With an impressive growth and a significant market share, as reported by Wohlers Associates,[16] it stands as the leading technology in the field. This method works by selectively melting and bonding powder layer by layer using a laser, enabling the production of intricate, high-strength parts that are often beyond the reach of traditional subtractive manufacturing approaches.[17] LPBF has gained interest for its role in manufacturing ceramics, polymers, metals, and composites, particularly in high-value industries like aerospace, automotive, biomedical, and electronics. Using a high-energy-density laser, LPBF has the capability to fabricate fully dense, high-strength, net-shaped oxide ceramics.[18–21] Although LPBF is more costly than conventional methods, it is especially valuable in aerospace, biomedical, and automotive sectors, where performance justifies the expense. Unique applications, such as biodegradable implants,[22,23] heat-resistant coatings,[24] and load-bearing bone implants,[25,26] highlight LPBF's versatility. The technology also enhances material properties by producing dense, high-strength parts with minimal postprocessing. Recent interest in ceramic LPBF continues to grow, though in-depth research is necessary to address challenges. Innovations and new ideas for adding materials to oxide ceramics, control, and effective optimization of process parameters could help overcome issues like crack formation, rapid cooling, residual stress, thermal gradients, and porosity.

There are several parameters and physical features involved in the LPBF process such as focused laser power, laser spot size, scanning speed, scanning strategies, layer thickness, and particle size distribution, which significantly influence the melting behavior and microstructure of ceramic powder. Several excellent reviews and research articles on the fabrication of ceramics via the LPBF process have already been published.[3,27–30] However, most of the LPBF parameters are not explored very properly or need further analysis. While several reviews have examined the AM techniques including the LPBF process for ceramic parts manufacturing,[3,10,31–33] there is still a need to further explore and summarize the root causes of defects, such as surface roughness, spattering, porosity, and cracks, which are among the most prevalent issues in AM of ceramics. Additionally, the approaches to prevent these defects and their limitations need to be studied in more depth. Furthermore, an updated overview of the mechanical properties of LPBF-fabricated parts, as well as the latest advancements in modeling and simulation techniques, is required considering recent advances and research in

the topic. This review provides an overview and comparison of the most common AM techniques, highlighting both current challenges and the potential of each method. In particular, this review focuses extensively on LPBF for ceramics, discussing the latest research developments, including a detailed investigation of ceramic part defects. Additionally, an overview of mechanical properties, as well as advanced modeling and simulation techniques used for the AM ceramics, are explored. The review also addresses the ongoing challenges in the AM of ceramic manufacturing, along with potential future advancements, particularly in process optimization and defect prevention strategies.

2 | AN OVERVIEW OF CERAMIC AM TECHNIQUES

Over the past three decades, various AM techniques have been developed and tested for fabricating ceramic parts and components. These techniques, while still at an early stage of industrial adoption, demonstrate distinct strengths and challenges. Although the primary focus of this study is to review the LPBF process, laser material interaction, and its effects on fabricating ceramic parts, it is also important to consider and discuss LPBF in relation to other ceramic AM techniques. This broader perspective provides an understanding of LPBF's unique features, strengths, and challenges compared with other methods. Each AM method has its own set of processing conditions, material compatibility, resolution, and defect control mechanisms, which directly affect the final quality and performance of ceramic parts. For example, techniques such as stereolithography offer high resolution and surface finish but require extensive postprocessing to achieve the desired mechanical properties. Binder jetting (BJ) provides rapid production speeds but struggles with achieving full density, often necessitating secondary sintering processes. Direct ink writing offers simplicity and material versatility but is limited in precision and structural integrity compared with other methods. Meanwhile, selective laser sintering (SLS) and LPBF offer advantages in terms of material consolidation and complex geometries but face challenges with high-temperature gradients and inherent brittleness in ceramics. Table 1 summarizes key aspects of various ceramic AM techniques, such as resolution, postprocessing requirements, defect control, and processing conditions. This overview enables a clearer comparison and highlights the strengths and limitations of each method, allowing for a more informed decision when choosing an AM technique for ceramic parts. The primary focus of this paper remains on LPBF, particularly its process conditions and defect mitigation strategies, to provide a thorough understanding of this method for ceramic applications.

2.1 | LPBF of ceramics

Among AM technologies, LPBF is one of the advanced laser-based techniques, known for its capability to create high-precision, layer-by-layer structures by directing a high-power laser onto selected areas of a powder bed, as illustrated in Figure 1A.[53,54] Unlike SLS, which relies on partial fusing of material particles, LPBF achieves complete melting of the material, resulting in highly dense and mechanically robust parts.[55–58] While LPBF has been extensively developed for metals and alloys, achieving significant industrial applications,[59–61] its adaptation to ceramics has proven far more challenging. The inherent properties of ceramics, including low thermal shock resistance, brittleness, and high melting points, lead to elevated defect rates, such as cracking and porosity.[62,63] These issues have limited the adoption of LPBF for ceramic manufacturing and hindered its broader application. As research progresses, LPBF is gradually moving toward enabling the production of high-quality ceramic components with complex geometries and enhanced properties. Figure 1 provides an overview of the LPBF process and ceramic parts printed using this AM method.

The direct application of LPBF involves full melting of ceramic powder without binders, making it a single-step process. However, direct LPBF often results in high-temperature gradients and residual stresses, which lead to cracking due to the rapid heating and cooling of printed layers. This issue is particularly severe for ceramics due to their low thermal shock resistance. Despite these challenges, recent efforts have concentrated on addressing these challenges by focusing on process optimization and material development. Improvements such as optimizing laser parameters (e.g., power, scan speed, and energy density [ED])[36,64–66] and tailoring powder properties[67–69] (e.g., size distribution, absorptance), and mitigating thermal stresses caused by rapid heating and cooling cycles[70,71] have significantly advanced the LPBF of ceramics. The most common issues across these investigations involve challenges in crack formation and suppression, particularly due to the inherent brittleness of ceramics and composites, requiring careful optimization of process parameters like laser power, scanning speed, and material composition. Similarly, different factors affecting the ceramic components are involved in the LPBF process, including laser-powder interaction and laser energy absorption by powders, fast heating and cooling of powders, structural growth, and flow in the molten pool, which is hard to control at the same time.

TABLE 1 A summarized comparison of ceramic AM techniques, showcasing their materials, precision, postprocessing needs, defect management, and process conditions.

Technique	Material compatibility	Resolution and precision	Postprocessing	Defect control	Processing conditions	References
Laser powder bed fusion (LPBF)	SiC, Al_2O_3, ZrO_2, MgO, TiB_2	High-precision, complex geometries	Possible sintering, complex defect removal	High defect rates (cracking, porosity), ongoing research for improvements	High energy laser, temperature gradients, controlled powder bed environment	[34–36]
Direct energy deposition (DED)	SiC, ZrO, TiB_2, MgO Al_2O_3, ZrO_2, Al_2O_{3-}, ZrO_{3-}, Y_2O_3	Moderate resolution, limited detail on complex geometries	No postprocessing required for large parts, may require cleaning	Moderate defect control, limited by material brittleness	Laser or electron beam melting, multiaxis deposition	[37–39]
Binder jetting (BJ)	SiC, Al_2O_3, ZrO_2, MgO, WC	Good resolution for small parts, limited detail for large geometries	Requires curing, sintering, or drying	Porosity control, limited precision, rough surface finish	Binder deposition, material powder bed, room temperature	[40–42]
Robocasting (RC)	Al_2O_3, ZrO_2, SiC, TiO_2	Moderate resolution, good for medium-sized structures	Requires sintering and postprocessing for mechanical property enhancement	Defect-free parts possible but requires precise slurry formulation and sintering	Extrusion of slurry, drying, curing	[43]
Fused deposition modeling (FDM)	Al_2O_3, ZrO_2, SiC, TiO_2 B_4C, SiOC + thermoplastic binders	Moderate resolution, suitable for medium and large geometries	Requires sintering, potential binder removal	Prone to porosity and cracking, requires postprocessing for defect reduction	Extrusion of thermoplastic filaments, melting, solidification	[44, 45]
Stereolithography (SLA)	Al_2O_3, ZrO_2, SiC, TiO_2, MgO + polymer binders	High resolution, limited by material constraints	Postcuring, sintering, binder removal	Porosity, shrinkage, and cracking issues, ongoing research	UV light-based curing, room temperature	[46–48]
Shape deposition manufacturing (SDM)	SiC, Al_2O_3, ZrO_2, MgO, Si_3N_4	High precision, good for complex geometries	Requires sintering and postprocessing	Limited defect control, material consistency is key	Layer-by-layer deposition of material, binder curing	[49–51]
Photochemical additive manufacturing (PAM)	Preceramic polymers	High precision, suitable for intricate geometries	Requires curing, sintering, or additional light treatment	Limited defect control, ongoing research to address challenges	Photochemical curing of resin layers, UV light exposure	[52]

2.1.1 | LPBF key process parameters and their effects on ceramic

The LPBF process relies on a precise balance of key parameters and physical characteristics, including laser power, spot size, scanning speed, scanning strategy, layer thickness, and particle size distribution. These factors fundamentally influence the melting behavior and microstructural development of ceramic powders. The LPBF system is typically composed of three main parts: the laser and scanning unit, the powder bed, and the powder spreading mechanism, each contributing uniquely to the precision and quality of the final ceramic product.

The laser system is the most important part of the LPBF process, responsible for selectively melting and fusing powder particles layer by layer to create a 3D object. Laser irradiates the surface of the powder bed based on the layer's cross-sectional data, with the absorbed energy being converted into heat that dissipates through the material, causing powder particles to melt and solidify into the desired shape.[76] The efficiency of this process largely depends on the material's ability to absorb the laser's energy as different materials have varying energy absorption characteristics.[77,78] In addition, various physical effects and associated phenomena, as illustrated in Figure 2, play a critical role in influencing the melting

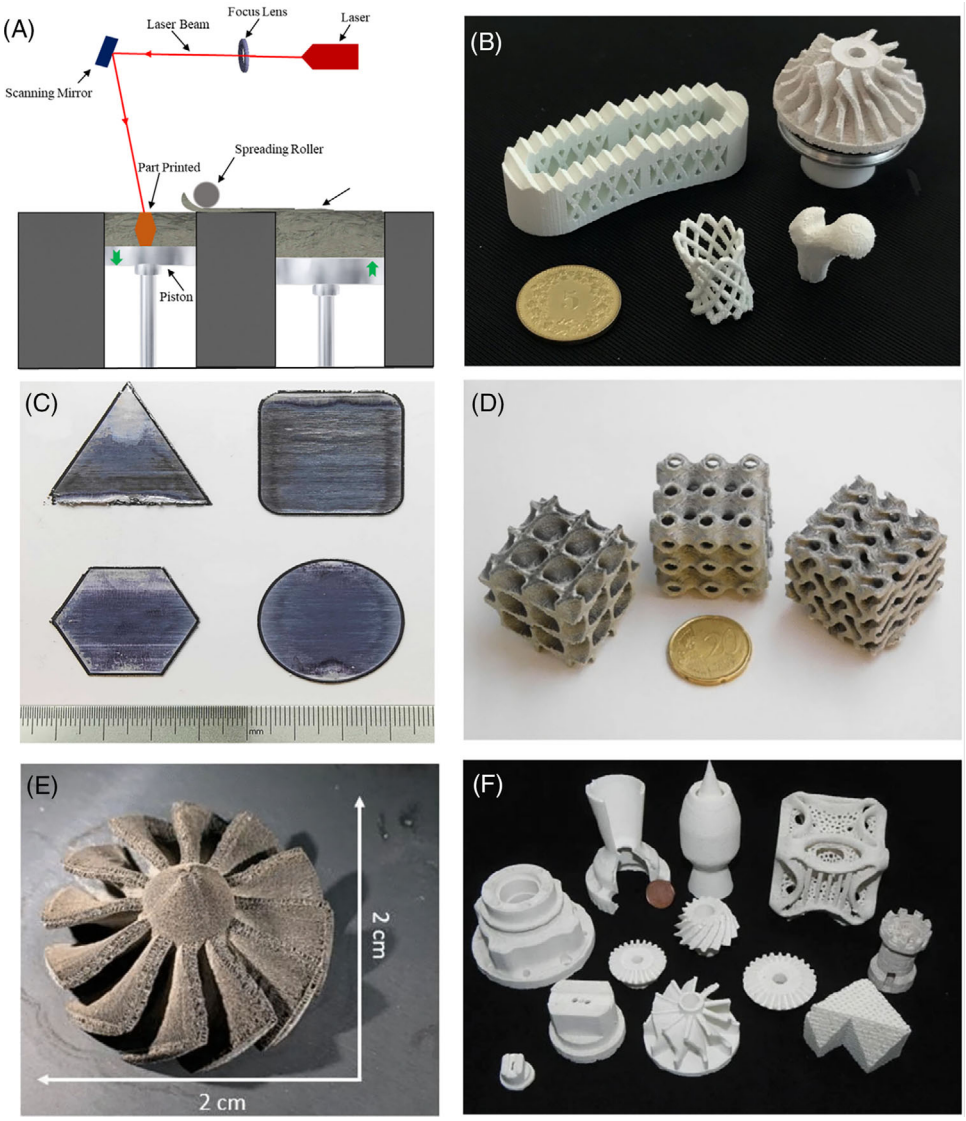

FIGURE 1 (A) Schematic illustrating the LPBF method, (B) Al_2O_3/ZrO_2 ceramics parts,[72] (C) $Al_2O_3/GdAlO_3/ZrO_2$ ternary eutectic ceramics of different shapes,[73] (D) alumina lattice structures, (E) SiC turbine part, and[74] (F) pure alumina parts.[75]

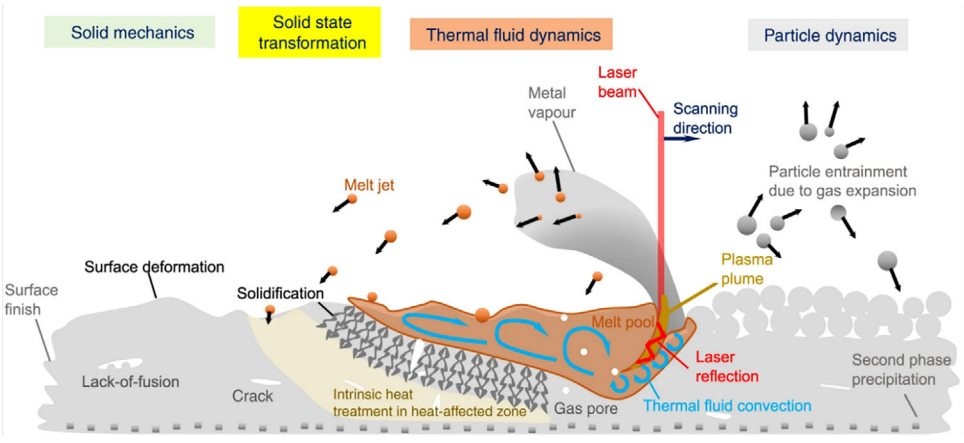

FIGURE 2 Schematic representation of molten pool dynamics during the LPBF process, illustrating key phenomena such as melt jet formation, thermal convection, gas pore generation, particle entrainment, plasma plume behavior, and surface deformation, emphasizing their influence on process stability and part quality.[85]

process and the manufacturability of ceramics. Therefore, selecting an appropriate laser source and optimizing the parameters is crucial. Fiber lasers, Nd: YAG, and CO_2 lasers are generally used in the LPBF process, which has distinct and notable effects on the experimental materials. Nd lasers, operating at around 1.06 μm, are suitable for metals and carbide ceramics like SiC due to their efficient energy absorption at this wavelength, enabling precise and rapid melting. CO_2 lasers, with a longer wavelength of 10.6 μm, are more effective for oxide ceramics, such as Al_2O_3, TiO_2, and ZrO_2, which absorb better in the far-infrared region. Additionally, fiber lasers, also operating near 1.06 μm, have become popular due to their high efficiency, superior beam quality, and flexibility, making them particularly suitable for high-precision metal processing and intricate geometries.[79,80] The choice of laser system impacts not only the melting efficiency but also the thermal gradients, solidification behavior, and microstructural evolution, all of which are crucial for achieving the desired mechanical properties and overall quality of the final part.[81]

Due to the high thermal and residual stresses created by higher ED during the LPBF process, several part defects are developed in ceramics. Considering the complex interaction between laser and ceramic powder and their influence on the defect's formation, the ED and size of the laser spot are imperative to consider. A smaller laser spot size results in more concentrated energy, leading to higher energy absorption and a narrower area of exposure.[82,83] Simultaneously, a smaller spot size lengthens the manufacturing time required to cover an area. Besides, ED is dependent on laser power and scan speed, which are the critical laser parameters of great significance in the LPBF laser system and directly affect the molten state of ceramic powders. Both laser power and scan speed show a much more dominant role than other parameters in the thermal behavior and shaping of the melting pool, initiation of cracks, dendrite growth, porosity, and grain size development.[35,36,84]

The laser scan strategy is one of the key parameters that may be utilized to control certain flaws and their detrimental impacts in ceramics.[86,87] Changing scanning strategies has a significant impact on heat transfer, powder melting, grain structure, and solidification.[88] The industry's urgent need for high-performance AM products drives the research for finding the optimized scanning strategy. Researchers have investigated various scanning strategies and their influences on the internal structure, mechanical properties, surface roughness, and residual stresses of LPBF parts. Ali et al.[89] studied the influence of various laser scan strategies and explored that adjusting the size and orientation of the scan vector length, scanning sequence, and rotation of each successive layer could lead to a constructive and remarkable combination of scanning strategies. However, numerous parameters are linked with the scanning method, making it a complicated matter to understand its real effects on the LPBF components. In the LPBF process, the two primary laser scan methods, island scanning, and zigzag scanning were widely used for ceramic sample manufacturing.[36,66,71,90,91] By carefully adjusting the laser scan methods, the components may be printed with a more uniform structure and the fracture density can be decreased. The previous research found that the "island" scanning greatly influences the grain structure of the material while the zigzag scanning strategy can help to reduce component distortion, improve the part's manufacturing quality, and may help to uniform residual stress distribution[71].

Recent investigations highlighting the key process parameters and their impact on the ceramic LPBF process and part quality are summarized in Table 2. Besides investigating the typical laser parameters, which included laser power, scanning speed, scanning strategy, and hatch spacing, a novel research focus in the LPBF process has emerged as laser beam shaping. The research on laser beam shaping explores how different beam profiles can significantly affect the processing of materials, their microstructure, and build rate.[81,92–95] Traditional Gaussian laser beams, commonly used in LPBF, tend to concentrate energy at the center, leading to steep thermal gradients that can result in cracking, residual stresses, and poor surface quality, especially in brittle materials like ceramics. These challenges have prompted the investigation of alternative beam shapes, such as top-hat, elliptical or donut-shaped profiles, which distribute energy more uniformly across the irradiated area and produce wider melt pools rather than creating keyholing, as illustrated in Figure 3. This more even energy distribution can reduce thermal stresses, improve powder melting behavior, and enhance the overall quality of the parts that are proven for metal material.[96,97] However, there is a need to deeply investigate the options of different laser beam shapes for printing ceramics, which are expected to reduce several defects associated with the Gaussian beam profile, such as keyholing, spattering, and porosity. Ceramics are prone to thermal stresses due to their low fracture toughness and high thermal expansion mismatch. The sharp thermal gradients caused by Gaussian beams intensify these stresses, promoting crack initiation and propagation. In addition, lack of fusion (LOF) defects can be produced when the surrounding powder particles are not melted adequately for the concentrated beam shape. The approach of using alternative beam profile, which has shown promise in recent investigations with metal materials,[98–100] offers a potential solution to the limitations associated with the conventional Gaussian beam profile. By optimizing the beam shape, such as switching from Gaussian to ring shape, it is possible

TABLE 2 Key process parameters and their impact on ceramic LPBF process and part quality.

Reference	Material	Parameter	Impact on ceramic LPBF process and part quality
Zhang et al.[64]	$RE_3Al_5O_{12}$ HEOCs	Scanning speed (40–120 mm/s)	• Density increased to 97.83% at 60 mm/s with moderate scanning speeds • Grain morphology transformed from equiaxed to ladder-like with increasing speed • Pore types varied with speed: spherical pores at low speeds, irregular pores at high speeds
Xiong et al.[118]	Al_2O_3–ZrO_2	Laser defocus distance (−3 to +3 mm)	• Transition from cellular-like to eutectic colony structure • Refinement of grain size • Improved relative density and mechanical properties • Fracture toughness peaked at 8.04 MPa $m^{1}/^{2}$
Zhang et al.[91]	Al_2O_3–ZrO_2	Scanning speed (70–120 mm/s)	• Influenced stress distribution; vertical cracks suppressed at optimal speed (100 mm/s) • Enhanced crack resistance with cellular microstructure
		Hatch spacing (50–175 μm)	• Controlled molten track overlap and temperature gradients • Repaired parallel cracks and inhibited vertical crack formation
		Scanning length (3–11 mm)	• Shorter lengths (3 mm) suppressed parallel cracks • Reduced thermal stress accumulation
Maurya et al.[107]	TiC-430 L-FSS	Preheating and melting scan energy density	• Lower energy density led to finer TiC phases and reduced residual stress; higher energy density caused coarser microstructures and more defects
		Scan speed during preheating (PHS)	• Lower scan speeds increased preheated bed temperatures, causing thermal residual stress and cracks • Optimized parameters achieved finer microstructures with lower porosity, resulting in the best combination of hardness (1218 HV) and fracture toughness (20.4 MPa $m^{1}/^{2}$)
Fang et al.[119]	3Y–ZrO_2	Scanning spacing (0.113–0.2 mm)	• Smaller spacing led to higher concavity and dimensional accuracy deterioration; optimal spacing improved surface morphology
		Scanning strategy (island, linear)	• Island scanning achieved highest dimensional accuracy (~184.573 μm height difference) and reduced powder spattering and warpage
		Double powder layering vs. single layering	• Double powder layering improved hardness (1258.2 HV, +15.7%) and nanoindentation modulus (85.18 GPa, +53.6%); reduced pore defects
Ullah et al.[120]	TiO_2	Laser power (80–170 W)	• Higher laser power improved melting behavior, resulting in refined microstructures and reduced porosity; optimal results at moderate power (120 W)
		Scanning strategy (zigzag, island)	• Island strategy produced only horizontal cracks and reduced spattering • Zigzag produced both horizontal and vertical cracks with spattering
Wilson-Heid et al.[121]	ZrC	Layer height (30–80 μm)	• Higher layer heights led to reduced density and increased porosity • Optimized layer heights facilitated better bonding and structural integrity
		Powder feedstock (−100 vs. −325 mesh)	• Spherical powder (15–45 μm) improved spreading and bonding • Finer powders (<2 μm) caused inconsistent layer deposition and porosity
		Build plate heating	• Potential to reduce cracking and improve layer bonding if heated above the ductile-to-brittle transition temperature (725°C)
Peters et al.[122]	SiC, Si_3N_4, and HfC/SiC	Processing gas (100 vol% CH_4, NH_3)	• CH_4 favored SiC and HfC/SiC formation; NH_3 facilitated α/β-Si_3N_4 synthesis with high yield (97.7 wt%)
		Energy density (8–58 W/mm^2)	• Higher energy density achieved better phase conversion • Low laser power facilitated uniform layer thickness and microstructural continuity
Liu et al.[123]	Al_2O_3/GAP /ZrO_2	Laser energy density (LED, 62.5–125 J/mm^2)	• Individually adjusting laser power or scanning speed improved melting quality; simultaneous adjustment caused irregularities and variations in melting dimensions.
		Laser power (100–400 W)	• Higher laser power significantly increased melting dimensions and forming quality compared with changes in scanning speed
		Scanning speed (48–192 mm/min)	• Adjustments affected LED impact less significantly than laser power; excessive speed caused wave-like melting inconsistencies

(Continues)

TABLE 2 (Continued)

Reference	Material	Parameter	Impact on ceramic LPBF process and part quality
Abdelmoula et al.[124]	Al_2O_3	Scanning speed (100–400 mm/s) Laser power (210 W)	• Higher speed (400 mm/s) achieved a relative density of 94.5%; improved surface quality and reduced defects compared with lower speeds • Optimized with scanning speed and hatching space to enhance relative density and minimize porosity

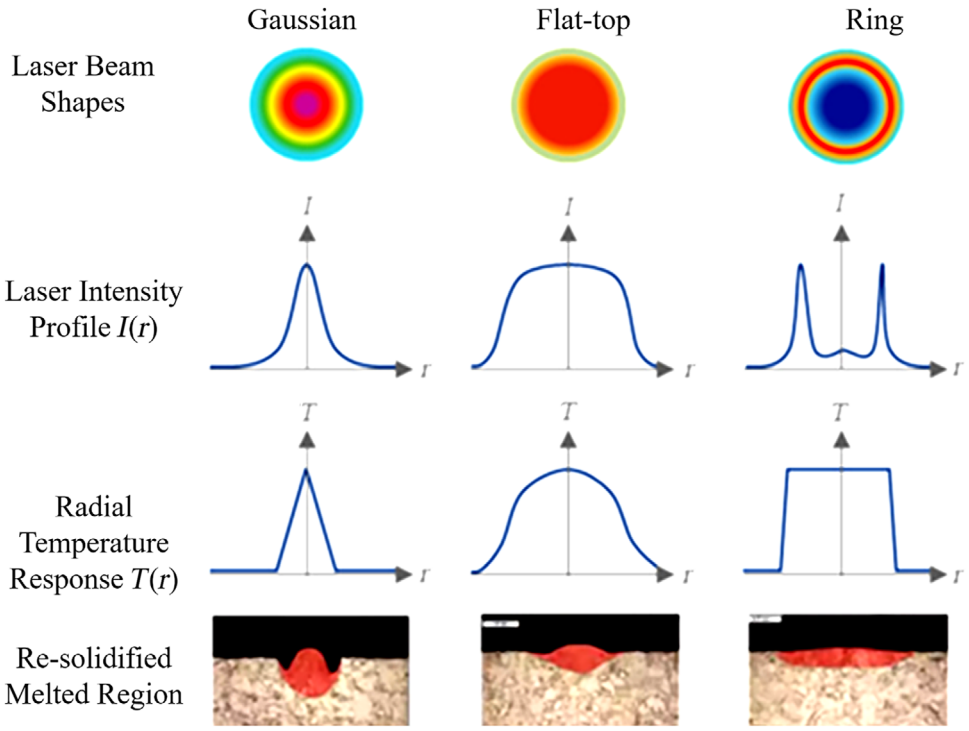

FIGURE 3 Comparison of laser beam shapes (Gaussian, flat-top, and ring) with corresponding laser intensity profiles, radial temperature responses, and resolidified melted regions. The illustration highlights how beam shapes influence energy distribution and melt pool geometry in the LPBF process.[101]

to achieve more controlled heat input, better melt pool dynamics, and ultimately, a more reliable LPBF process for complex materials like ceramics.

2.1.2 | Powders and layer thickness

In addition to the laser parameters, the properties and specifications of the powder also play a significant role in the production of the part through the LPBF process. The size, shape, and distribution of the powder particles have a significant influence on the part characteristics and laser melting efficiency.[102–105] In LPBF, powder flowability and powder layer density are thought to be the link between powder and part qualities. Material flowability and particle distribution on the powders bed are critical for the process. The flowability of the powder has a strong effect on the formation of a uniform layer and the absorption of laser energy. In addition, the powder size shows a key role in determining the packing density and flowability of the powder bed. The size distribution of particles describes the relative number of particles (by mass) concerning their size ranges. Previous studies have shown that smaller particles improve the surface smoothness and density of the powder bed, leading to finer features and higher part resolution. However, powders that are too fine can lead to issues such as agglomeration and poor flowability, hindering the uniform deposition of powder layers and affecting the stability of the process.[102,106–109] Powder shape is another important factor that may influence the uniform layer deposition and surface roughness of the final part. Spherical particles are generally preferred due to their superior flowability and packing characteristics, which promote a more consistent layer deposition during LPBF. In addition, spherical powders also reduce the formation of defects, such as voids and incomplete fusion, as they allow for more even heat distribution during laser irradiation. In contrast, irregular-shaped particles, common in some ceramic powders, can

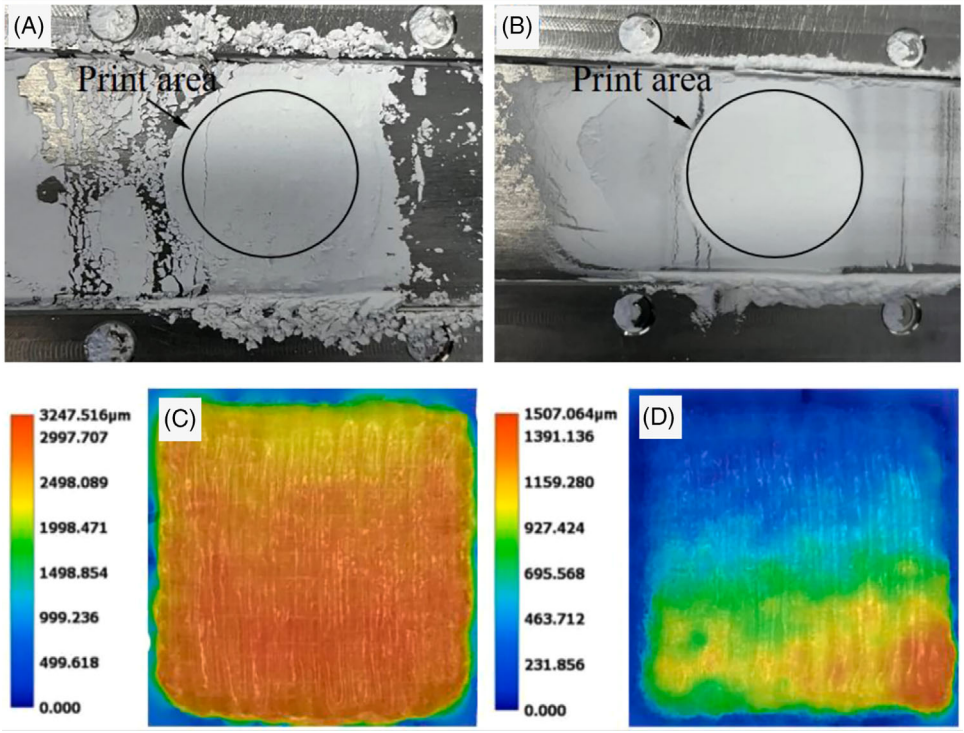

FIGURE 4 Morphology comparison of Al_2O_3 powder states and their corresponding specimens: (A) Irregularly shaped powder; (B) spherically shaped powder. Height maps illustrating surface profiles of Al_2O_3 specimens: (C) specimen formed from irregular powder; (D) specimen formed from spherical powder.[112]

cause inconsistent layer thickness and lead to pore formation, thus influencing the part quality and mechanical strength of the final parts.[75,110,111] A study conducted by Zhang et al.[112] on optimizing powder morphology in Al_2O_3 ceramics clearly illustrates the significant influence of particle shape, as shown in Figure 4. However, there is limited literature available on the effect of particle size in the LPBF of ceramics, indicating a need for in-depth investigation to better understand its impact on process performance and part quality.

Uniform layers of small thickness are more desirable to absorb sufficient laser energy from the laser beam. The studies[113–116] on the effect of layer thickness in LPBF process shows that thinner layers generally result in finer resolution and better surface finish, as the laser can more precisely melt each layer, leading to fewer defects and a more uniform microstructure. Studies have shown that using layer thicknesses in the range of 20–50 µm for ceramics can improve part accuracy and reduce surface roughness.[34,36,91] Thinner layers also facilitate better control over the thermal gradients, reducing the risk of cracking and residual stresses, which are common issues in ceramic LPBF due to the material's sensitivity to temperature fluctuations. However, while thinner layers improve part resolution and surface quality, they may also extend the build time, as more layers are required to complete the part. This relationship between build speed and part quality is a key factor in choosing the appropriate layer thickness for ceramic parts. Thicker layers, on the other hand, increase the build speed but can lead to issues such as incomplete melting between layers, poor layers bonding, increased porosity, and reduced mechanical strength, as the laser may not fully penetrate the thicker layers, leaving some particles unmelted. Furthermore, layer thickness affects the heat transfer between layers. In thicker layers, heat is distributed less evenly, which can cause variations in the microstructure and mechanical properties.[114,117] For ceramics, this is particularly problematic, as uneven heat distribution can worsen the formation of cracks and defects. Thinner layers help to control these issues by allowing for more consistent heat application across each layer, leading to improved part density and fewer internal defects. However, an in-depth study on the effect of layer thickness in LPBF of ceramics is necessary to thoroughly understand its impact and to determine the optimal layer thickness for each specific ceramic material.

2.1.3 | Common part defects in ceramic LPBF

AM techniques also have some limitations and challenges. The formation of defects is a serious shortcoming and

challenge in the ceramic parts produced by the LPBF process. In addition to the various LPBF process parameters such as laser scanning speed, hatch distance, laser power, ED, layer thickness, powder characteristics, and experimental environment, there are several other factors that may contribute to the complexity of the LPBF process and affect the surface quality of the part, such as laser energy transmission and absorption rapid heating and cooling of powders, structure evolution, and high-temperature gradient. These factors are difficult to control or optimize simultaneously and have a significant impact on the manufacturing process, resulting in several defects and flaws. These defects include fractures and microcracks, which arise due to the inherent brittleness of ceramics and the rapid thermal gradients during processing. Porosity, which results in a porous structure or individual pores, can lead to reduced density and compromised structural integrity. Other common defects, such as dendritic formations, columnar grains, and surface roughness, can further weaken mechanical properties. Additionally, defects like hot and cold ejected spatters, the balling effect, and the formation of solidified droplets on the surface can lead to nonuniform part dimensions and poor surface finish. Figure 5 illustrates the overall appearance of the various defects mentioned, which were observed in the ceramic parts produced with the LPBF process. Understanding and mitigating these defects are critical for improving the reliability and quality of ceramic components produced using LPBF. The applications of LPBF technology are severely limited due to the defects mentioned above.[125–127] Therefore, because ceramics are naturally brittle, have a low thermal shock resistance, and are overly resistant to treatment and heat conductivity, manufacturing ceramics using this method is more challenging. This part overviews the recent research on key part defects found in the ceramic parts produced by the LPBF process.

Formation of cracks

Crack formation is one of the most common part defects in ceramic LPBF, severely limiting their uses and applications.[86,129] Cracks in LPBF of ceramics, such as Al_2O_3, ZrO_2, and other ceramic composites, are primarily caused by thermal stresses because of the rapid cooling of the printing layers, which induces large temperature gradients in the material. Ceramics, being brittle materials, are highly sensitive to cracking when subjected to tensile stresses during solidification. Most of the LPBF machines use a Gaussian laser beam profile, which produces the highest energy at the center point and melts a localized region of the powder bed, and as the molten pool solidifies, shrinkage and thermal contraction can cause cracks to form either within the melt pool or between adjacent layers. Cracks negatively affect part quality in multiple ways, such as the micro cracks reducing mechanical integrity by acting as stress concentrators, which can lead to premature failure under mechanical or thermal loads.[12,91] Cracks also reduce density of the parts and can compromise the dimensional accuracy of parts, as observed in multiple LPBF ceramic studies. For example, the presence of longitudinal and transverse cracks due to tensile and shear stresses was identified in Al_2O_3/ZrO_2-based components, leading to a decline in overall mechanical properties such as toughness and strength.[130] Additionally, cracks in the interlayer can propagate during subsequent laser passes, leading to layer delamination and overall structural weakness of the printing components.[20] Consequently, crack prevention in the LPBF process has become a serious concern. There has been some prior research on the causes and prevention approaches for crack formation in LPBF ceramic components. Zheng et al.[71] separated cracks into two types: transverse cracks and longitudinal cracks. Cracks that are parallel to the laser scan direction are known as longitudinal cracks (L-cracks), whereas transverse cracks (T-cracks) are perpendicular to the laser scan direction, as shown in Figure 6.

Ullah et al.[90] investigated several causes behind the transverse cracks, longitudinal cracks, and cracks bifurcation. The production of transverse cracks can be caused by a number of factors, including an exceedingly high-temperature gradient, residual and thermal stresses, large pores, or inadequate melting of the deposited powder layers. Transverse cracks were also found to be produced by external cracks and substrate thermal expansion. High viscosity, weak bonding and tensile strength, and limited flowability, characterize the partially melted or unmelted powder.[131,132] As a result, thermal stresses are difficult to release even with minor deformation, resulting in the creation of transverse cracks. Research into the effects of laser parameters on cracks formation and propagation in LPBF processes has consistently shown that both laser power and scanning speed play critical roles in crack generation. The correct combination of these two parameters is necessary, as it directly influences the laser ED delivered to the powder layers. High laser power combined with slow scanning speed can cause excessive heat accumulation, leading to large thermal gradients and increased cracking. Conversely, low laser power and high scanning speeds might lead to insufficient melting, causing LOF defects and stress concentration, which can also result in cracks.[34,71,91] Therefore, optimizing laser power and scanning speed to maintain an appropriate ED is crucial for minimizing crack formation and improving the quality of the printed parts.

In a study, Liu et al.[86] thoroughly analyzed the characteristics and formation mechanisms of crack defects in various ceramic AM processes and proposed a few

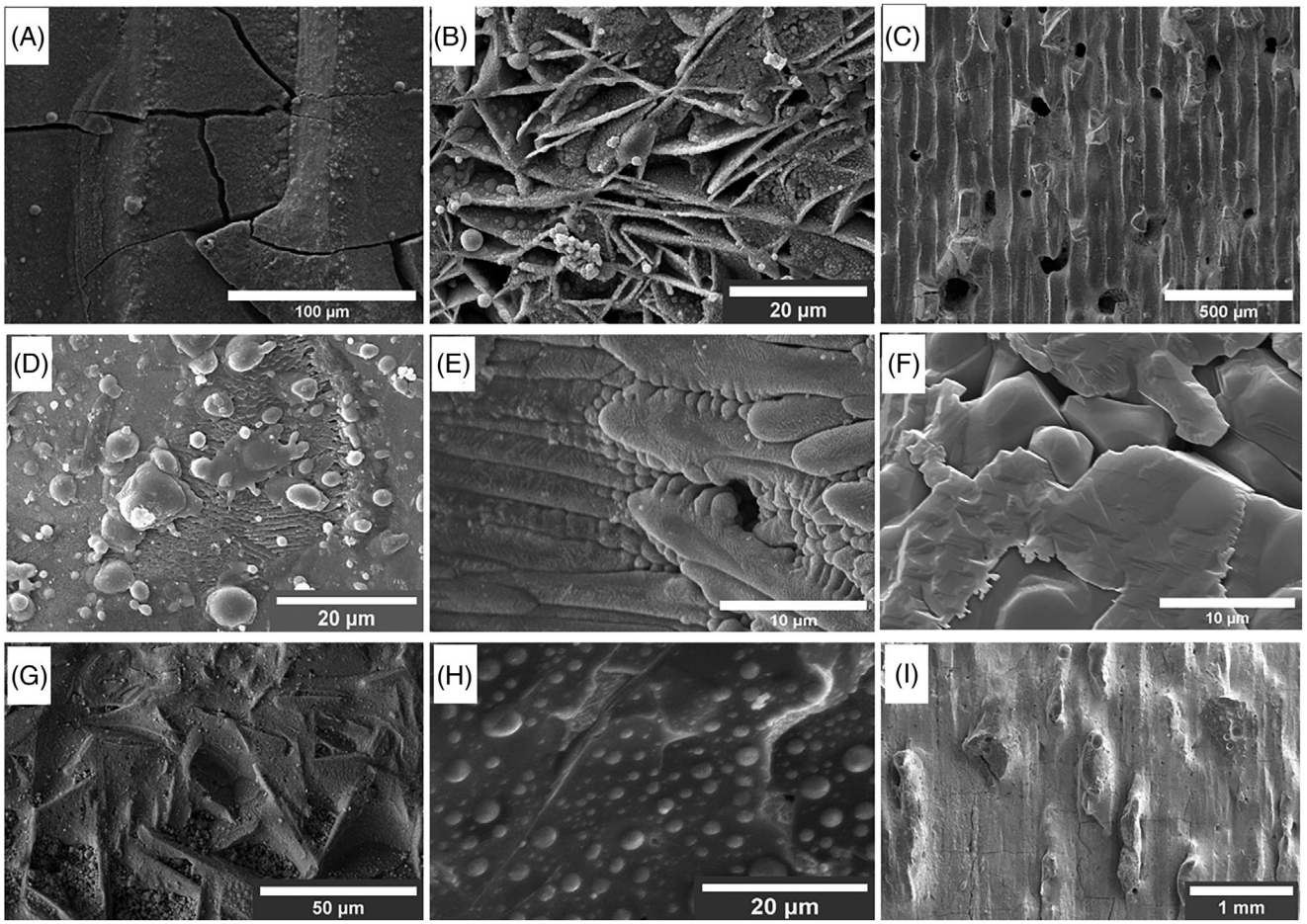

FIGURE 5 Part Defects in Ceramics (A) Fractures and Microcracks (B) Porous Structure (C) Pores (D) Hot Ejected Spatters (E) Dendrites (F) Columnar Grains (G) Surface Roughness (H) Balling Effect (I) Cold Ejected Spatters[36,90,128]

significant crack inhibition methods. In the laser-based ceramic AM process, an appropriate combination of laser power and scanning speed can considerably reduce the energy absorbed by the ceramic powder, lowering the internal stress of the part. In addition, by optimizing the process parameters and material composition, the flow of the molten pool is regulated and the developing thermal stress in the molten pool is released, resulting in grain refinement and toughening, which ultimately improve the crack initiation and growth resistances. Similarly, Huang et al.[133,134] utilized a thermal model to study the solidification behavior and crack mechanisms in ceramics. Their investigation highlighted the influence of varying laser parameters on cracking characteristics, demonstrating the critical role of controlled microstructure and parameter optimization in managing crack morphology and distribution.[133,134]

Besides laser parameters, Shen et al.[73] revealed in a study that layer thickness and number of layers also have a significant effect on crack formation and propagation, as demonstrated in Figure 7. Crack density tends to decrease as the number of layers increases, with the most significant crack propagation occurring in the first three layers. At higher layers, cracks become less prominent and may even begin to heal or deflect, especially by the fourth layer. However, cracks formed in the initial layers may expand further based on the original defects, and cracks in cross-sections often deflect at an angle relative to the scanning direction. Ceramics have low fracture toughness and high resistance to heat conductivity; therefore, microcracks are easily formed in the printing parts, which causes large fractures. Therefore, improving the fracture toughness is required to prevent cracking. Previous studies have explored that the addition of ZrO_2 to Al_2O_3 is an effective way for improving fracture toughness through bridging the cracks and deflection mechanisms.[135,118,136] Similarly, addition of SiC and MgO to alumina was also found to be effective in the preventions of surface defects including cracks.[36,137,138] Chen et al.[45] investigated the significant impact of particle size on the quality and performance of bulk ceramic samples, as well as its role in fracture inhibition. Their findings revealed that smaller particles contribute to substantial volume shrinkage and reduced porosity, resulting in enhanced mechanical performance. However, they also

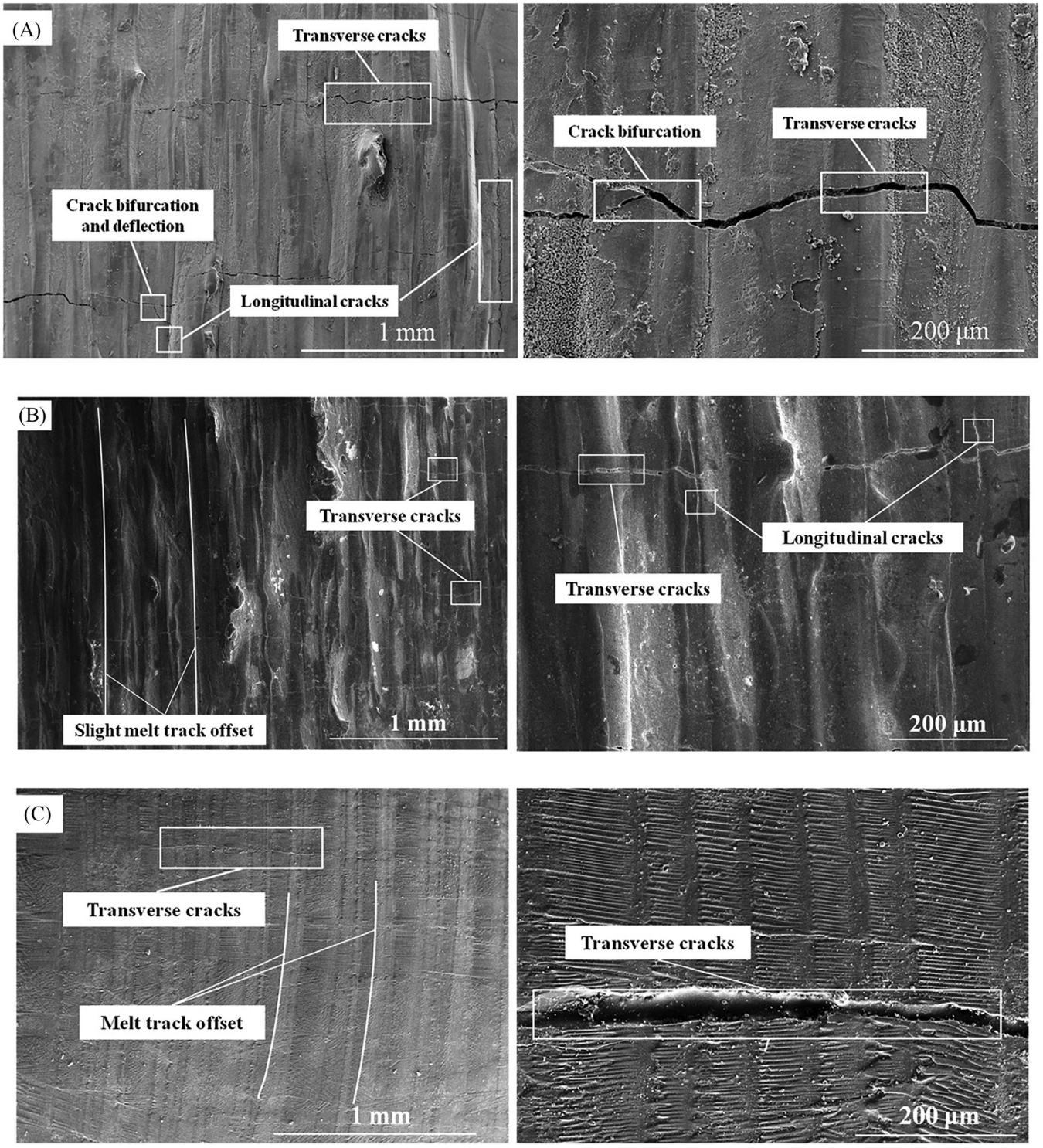

FIGURE 6 Experimental results showing the formation of transverse and longitudinal cracks in ceramic LPBF. Micromorphology of zigzag Al_2O_3 samples under laser powers of (A) 100 W, (B) 120 W, and (C) 210 W and a scanning velocity 90 mm/s. (Reproduced with permission from Ref. 71, Copyright Elsevier, 2019.)

observed the formation of surface microcracks due to the large volume shrinkage. These microcracks were notably mitigated through the sintering process, demonstrating that part sintering is an effective method for eliminating such defects.

Maurya et al.[107] applied a dual laser scanning technique, using separate laser parameters for preheating and melting stages to produce ceramics without cracks. The preheating scan minimized thermal gradients and residual stresses, while the melting scan ensured adequate

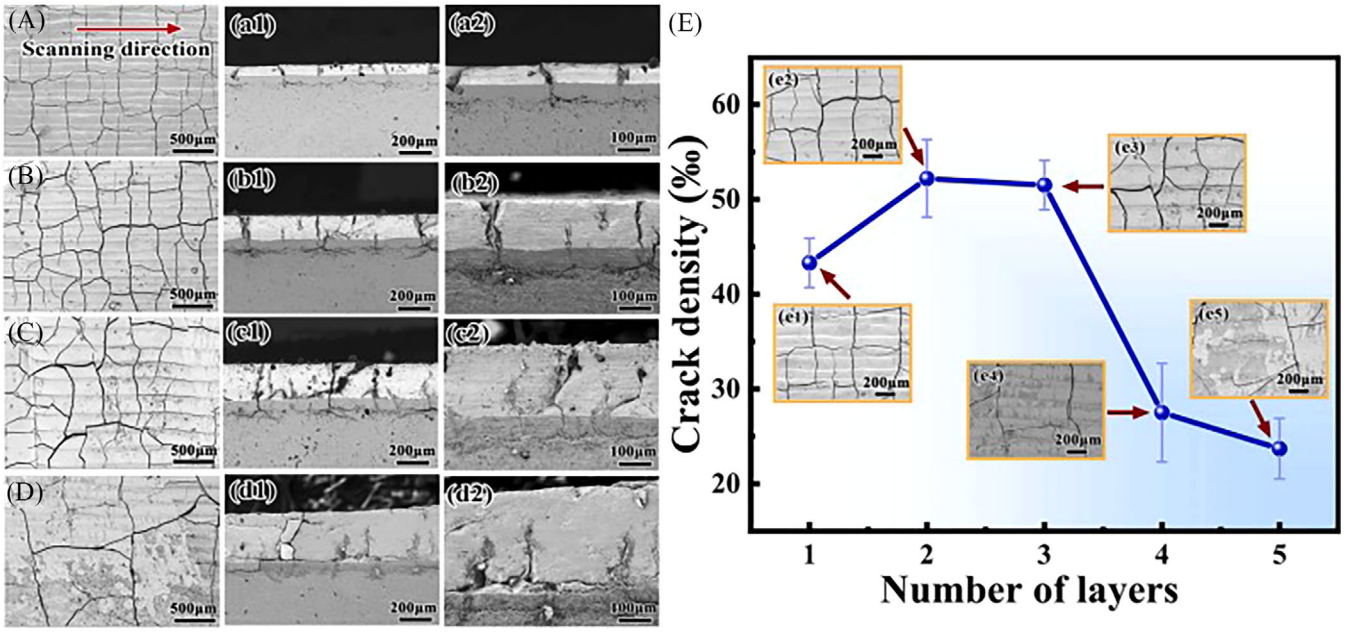

FIGURE 7 Crack distribution across various layers on the top surface and in the cross-section of the specimens: (A–A2) first layer, (B–B2) second layer, (C–C2) third layer, and (D–D2) fourth layer; crack density for each layer is shown in (E). (Reproduced with permission from Ref. 73, Copyright Elsevier, 2023.)

densification and material bonding. Laser preheating was found to be an effective way of eliminating the presence of cracks since it lowers thermal residual stress, which results in as-built ceramic parts with good mechanical properties. Liu et al.[139] in another study explored the influence of high-temperature preheating on crack distribution. They concluded that the transformation of orderly cracks to small, disordered cracks is achieved through high-temperature preheating. Wilkes et al.[140] investigated the LPBF of ceramic powder and reported that crack-free ceramic parts could be manufactured by reducing the thermal stresses using high-temperature (1600°C) preheating. However, this approach has certain limitations, including suboptimal surface quality of the final component and a restricted maximum height of 3 mm for the fabricated sample. Similarly, postprocessing such as HIP[141] and annealing temperatures[142] were found to be very effective in coursing the microstructure and closuring the voids, resulting in improved fracture toughness.

Asif et al.[143] introduced a new approach of printing ceramics from metals by selective laser oxidation, which severally improved the melting condition of the powder and reduced multiple part defects associated with the poor melting of the powder particles including cracks and large fractures. In this method, Cu_2O was changed into CuO by high energy input of the laser beam in the oxygen environment. The same approach was applied by another researcher where TiO_2 was printed from Ti by selective laser oxidation, which showed some improvement in the defects controlling of the pure TiO_2 ceramic printing, as shown in Figure 8.[90] However, this approach also has some limitations, like controlling oxidation before and after applying the laser beam, risk of fire catching, thermal expansion of the substrate, and so on. Table 3 summarizes the major findings in recent research on the root causes of cracks and their prevention approaches. Although these mentioned research approaches reduced cracks and other parts defects to some limits in LPBF of ceramics, there is still needed to further investigate the problems to eliminate the microcracks such as advanced postprocessing techniques, research on materials, process optimization, and necessary modifications in the existing LPBF machines to meet the ceramic manufacturing requirements. The sorts of defects discussed in the following sections are some of the main origins of cracks that, if addressed first, may help to reduce cracks.

Porosity and spattering formation

The formation of pores during the manufacturing process is a significant factor contributing to cracks and other defects, which critically undermine the mechanical performance of the manufactured components. Porosity produced during the LPBF process is directly affecting the material's mechanical strength, density, and overall performance.[36,148,67] In ceramic components, where high precision, smooth surface and structural integrity are required, the presence of pores can lead to premature failure and reduced functionality by lowering the part

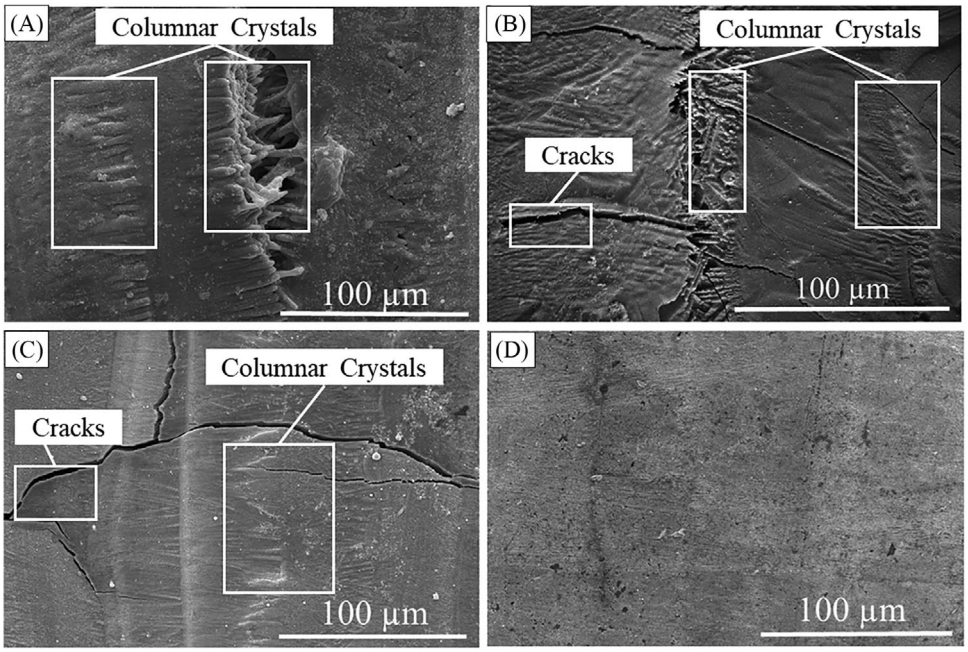

FIGURE 8 The effect of Ti content on TiO_2 surface morphology and cracks formation. SEM micromorphology of TiO_2 and (A) 0% Ti, (B) 3% Ti, (C) 5% Ti, and (D) 15% Ti at laser power 75 W and scanning speed 200 mm. (Reproduced with permission from Ref. 90, Copyright Emerald, 2020.)

density and facilitating the initiation of cracks, restraining the material's use in demanding industries like aerospace, electronics, automotive, and biomedical applications.[90,149] Understanding the underlying causes of porosity and implementing effective strategies to minimize its existence is critical to advancing the industrial adoption of ceramic LPBF. Although some porosity is unavoidable due to the inherent nature of the LPBF process and the physical properties of ceramics, extensive research has aimed to identify the key factors contributing to porosity formation, with the goal of developing more, productive reliable and defect-free manufacturing methods.[36,150,151,67]

In general, pores formed in the ceramic LPBF process are classified as spherical pores or gas pores and LOF holes, also known as irregular pores. LOF pores are generated when a few powder particles remain unmelted or incompletely melted (because of partial melting) as a consequence of smaller energy input during the laser melting and sintering process, while gas pores are formed as a result of entrapped gases either in the powder particles during the synthesis process or in the layers during the rapid melting and solidification.[152,153] The reported investigations[36,71,90,91] on porosity in ceramic LPBF show that pores formation is the major cause of cracks where most of microcracks in ceramics begin at the outer edges of pores and propagate, dividing into branches that induce crack bifurcation or link to further pores (Figure 9).

Zhiwen et al.[154] investigated the formation mechanisms and conducted the quantities analysis of pores in Al_2O_3–ZrO_2 ceramic. Their research categorized the pores in ceramic structures into four distinct types: intercrystallite pore, interlayer pore, intralayer pore, and shrinkage pore. Ullah et al.[90] reported that the irregular or uneven pores are big and gather around the edges of neighboring scan tracks, whereas the spherical gas pores are smaller and dispersed throughout the tracks. In their research, the source of pores formation was linked to the discontinuous melting tracks and melt pool's instability at reduced laser energy by lowering laser power. In addition, the cause of pore development in TiO_2 ceramics was connected to the discontinuous melting tracks and melt pool instability at lower laser energy levels. The number of pores seemed to be widely reduced by achieving sufficient melting of the powder using a high-power laser beam withing their certain ranges (100–150 W) and reduced scanning speeds (between 150 and 200 mm/s). In another study, Marattukalam et al.[155] studied the effect of varying laser power on porosity development in Zr-based bulk metallic glass, which supports prior findings and illustrates that adequate melting of powder at high energy input plays a critical role in preventing porosity. In a similar investigation by Lei et al.[156] shows that optimizing laser parameters, such as scanning speed and power, in ceramic AM can significantly reduce porosity and improve surface quality. Faster laser scanning speeds limit the saturation of molten material into surrounding porous regions, enhancing surface uniformity. Adjusting the line spacing between laser passes also helps refill voids, leading to smoother, denser ceramic

TABLE 3 Key references on recent studies of crack formation and prevention strategies in ceramic LPBF processes.

References	Materials	Major findings
Rehman et al.[36]	Al_2O_3 + MgO/SiC	• MgO and SiC additives improve surface finish and cracks prevention but higher amount (>30%) of these additives increases crack risk due to higher thermal gradients.
Ullah et al.[128]	Cu2O + CuO	• Higher energy input withing a certain limit improves melting behavior and prevent cracks formation. Optimization of laser parameters plays a critical role.
Zhang et al.[91]	Al_2O_3 + ZrO_2	• Optimized parameters reduced parallel and vertical cracks in Al_2O_3–ZrO_2 samples, with cellular structures offering higher crack resistance.
Pfeiffer et al.[144]	ZrW_2O_8 and $Al_2W_3O_{12}$	• The in situ formation of negative thermal expansion phases like ZrW_2O_8 significantly reduced crack formation in Al_2O_3 parts, with optimized phase ratios minimizing cracks further.
Zhang et al.[66]	Al_2O_3–ZrO_2	• Slower scanning speeds enhance ZrO_2 dendrite formation, improving toughness, but fine eutectic structures at high speeds reduce fracture toughness and increase cracking risk.
Chen et al.[45]	$BaTiO_3$	• Smaller particle sizes lead to better performance and reduced cracking in $BaTiO_3$ ceramics.
Maurya et al.[107]	CMC	• Preheating the powder bed reduces the thermal gradients and cracking in ceramic matrix composites (CMC) parts.
Kaya et al.[145]	Al_2O_3	• A novel preheating system for LPBF of alumina reduced cracking by enabling preheated powder before sintering, achieving over 80% density in printed samples.
Abdelmoula et al.[124]	Al_2O_3	• Higher scanning speeds improved alumina print quality, but cracking issues remained, suggesting the need for an efficient preheating system to address ceramic LPBF cracks.
Ur Rehman et al.[143]	Cu_2O	• Oxidation of Cu_2O into CuO by sintering and melting with high power laser beam shows improved melting behavior but crack formation needs careful energy control.
Wu et al.[146]	SiC-Si	• In Si/SiC Gyroid structures, uniform shrinkage leads to single crack propagation, while nonuniform stress distributions in graded structures cause multiple cracks.
Özmen et al.[147]	Al_2O_3–ZrO_2	• Direct LPBF of alumina-toughened zirconia achieved 96.7% density, but further optimization is needed to improve the crack pattern.
Wilson-Heid et al.[121]	ZrC	• ZrC exhibited intra and inter melt pool cracking, with crack reduction by using optimized powder feedstock and a heated build plate.
Shen et al.[73]	Al_2O_3/$GdAlO_3$/ZrO_2	• Tensile and shearing stresses during LPBF of Al_2O_3/$GdAlO_3$/ZrO_2 ceramics caused longitudinal and transverse cracks, with crack sensitivity increasing as more layers were added.

layers. These advancements maintain the crystalline phase of ceramics like Al_2O_3 while achieving over 90% relative density.

The input of sufficient energy to melt the powder properly by the laser beam plays an important role in controlling the porosity, but optimizing the laser parameters alone may not be sufficient to eliminate the pores completely, so, it is also important to focus on the material aspect rather than the focus on laser parameters only. The use of material additives, small powder particles with regular shapes, drying the presence of moisture on the surface of the particles, and layers of a small thickness are all likely to considerably reduce porosity, according to prior studies on porosity control in ceramics using the LPBF technique. Ur Rehman et al.[36] investigated the influence of MgO content on the porosity development in alumina ceramic, finding that the addition of 10% MgO significantly reduces the formation of pores in alumina, but increasing the MgO content to 60% produced poor surface and downgraded the printing parts, possibly due to the high melting point of MgO contents. The represented findings are shown in Figure 10. The same study also explored the effect of silicon carbide on the SLM/SLS process of alumina and found that the weight fraction of SiC had a substantial effect on the microstructure of the printed specimen. The experimental findings revealed that the addition of a lesser amount of 2% SiC powder inhibited most surface flaws, including the porosity formed in the samples.

The influence of laser defocus shift in ceramic LPBF was also studied, which shows a significant impact on keyholing, porosity and defect distribution in Al_2O_3–ZrO_2 eutectic ceramics. At moderate defocus levels, void defects are reduced, leading to higher relative density and improved material properties. However, as the defocus increases beyond a certain point, porosity begins to rise again, resulting in a decline in surface quality and overall

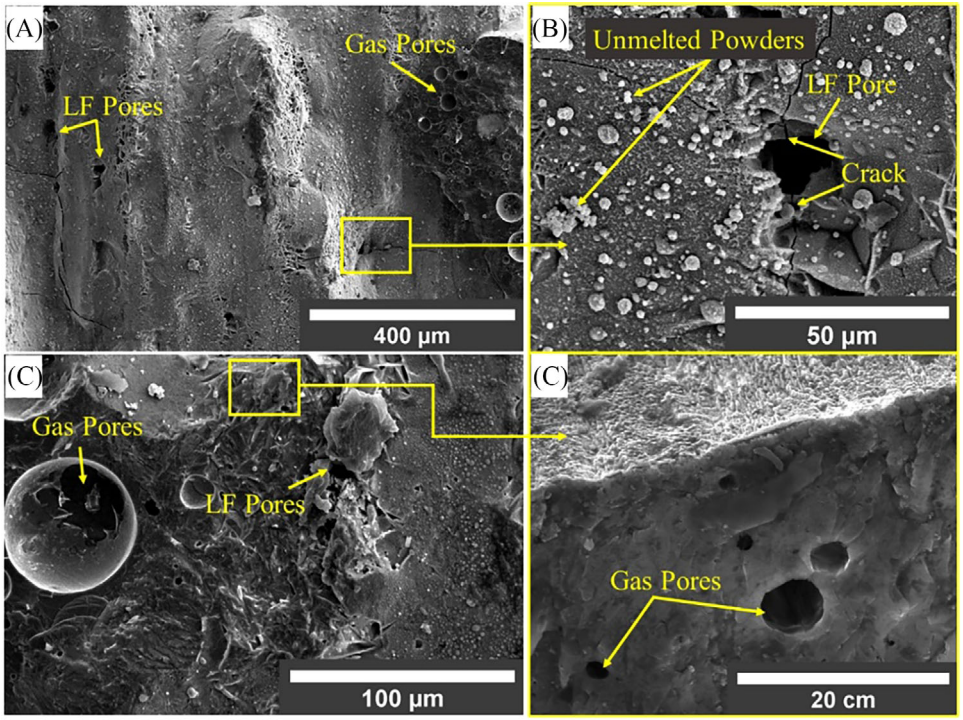

FIGURE 9 Formation of porosity and cracks initiation in Cu_2O ceramic with lower energy input (A and B) surface morphology. (B and C) Cross-section. (Reproduced with permission from Ref. 34, Copyright Emerald, 2022.)

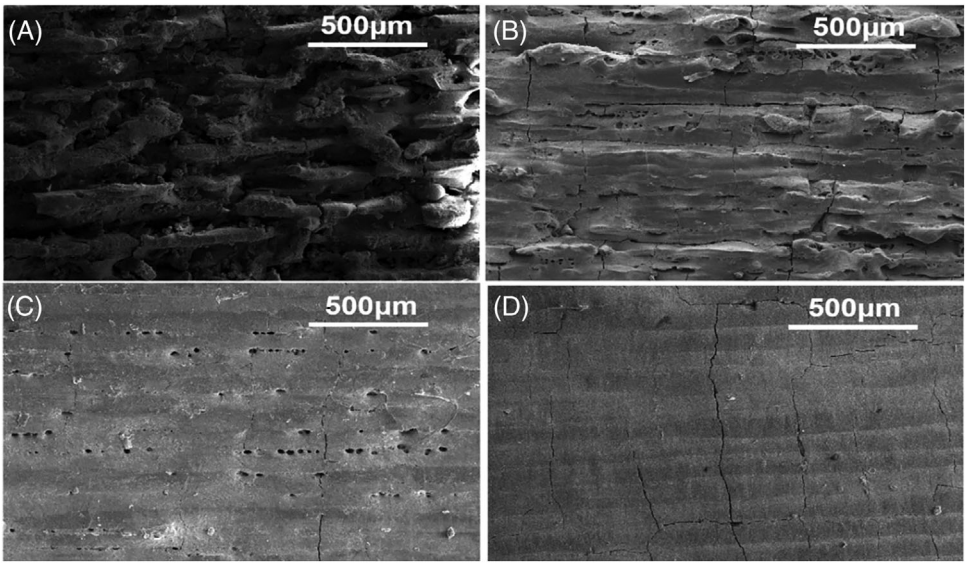

FIGURE 10 SEM images showing the effect of varying alumina (Al_2O_3) and magnesia (MgO) content on surface morphology and porosity at 70 W laser power: (A) 20% Al_2O_3, 80% MgO, (B) 60% Al_2O_3, 40% MgO, (C) 75% Al_2O_3, 25% MgO, (D) 90% Al_2O_3, 10% MgO. (Reproduced from Ref. 158, Copyright Frontiers, 2023.)

performance. This balance between reducing and increasing porosity highlights the importance of optimizing laser focus for achieving dense, high-quality ceramic components in LPBF processes.[118] A recent study[157] on single tracks revealed that porosity in Al_2O_3 by LPBF is primarily influenced by the interaction between the keyhole dynamics and the physical properties of ceramic. The formation of porosity seemed to be closely tied to the depth of the keyhole and the resulting distresses at the Ti/Al_2O_3 interface. As the keyhole penetrates deeper into the Al_2O_3

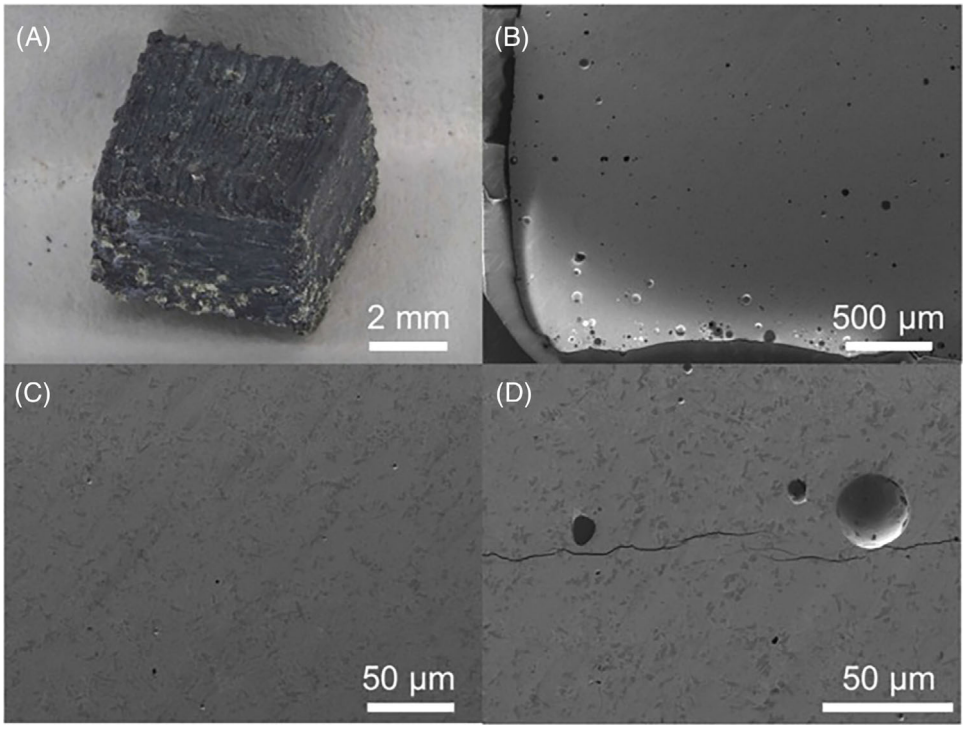

FIGURE 11 (A) Optical microscopy image showing the printed shape of the laser-manufactured specimen produced with 3.1 vol% coarse alumina (AA18) and 96.9 vol% spray-dried ZrO_2/WO_3 granules. (B–D) SEM images of cross-sections (top view) revealing the microstructure of the part. At higher magnification (D), a few cracks were observed, along with spherical porosity, likely caused by the local evaporation of tungsten oxide. (Reproduced from Ref. 144, Copyright Elsevier, 2024.)

substrate, the increased turbulence and instability in the melt pool create conditions conducive to gas entrapment and void formation. Additionally, the high viscosity of molten Al_2O_3, coupled with its low thermal expansion coefficient, affects the melt flow behavior, making it difficult for trapped gases to escape, further contributing to porosity formation. These findings show the need for careful control of laser parameters and keyhole depth to control or minimize porosity and improve the quality of the metal–ceramic interface in LPBF processes.

Pfeiffer et al.[144] revealed in their investigation that porosity in alumina structures produced by LPBF primarily caused by several factors, including incomplete sintering, material evaporation by keyholing, and spatter during the laser melting process. The spherical pores observed in the final parts were likely a result of localized evaporation of tungsten oxide in the composite particles, as shown in Figure 11. In addition, poor control of the laser power and keyhole formation contributed to inconsistent melt pool dynamics, leading to gas entrapment and pore formation within the alumina matrix. These findings highlight the importance of optimizing process parameters to minimize porosity and enhance the structural integrity of PBF–LB fabricated ceramics.

Besides laser parameters optimization and energy control, the postprocessing methods also play a significant role in reducing porosity. Azami et al.[159] produced an alumina and Fe–Ni (steel) alloy composite material using the LPBF method, showing the fine microstructure of the alumina matrix and the evenly distributed steel (Fe–Ni) particles. Although, microcracks and pores were found, which were eliminated by polymer impregnation and heat sintering. The printed parts that were passed through annealing at high temperature were found to have fine microstructures, lower porosity and improved fracture and interface characteristics.[160] HIP is a widely utilized postprocessing technique aimed at eliminating defects in parts, including lack-of-fusion, keyhole imperfections, surface roughness, residual stress, and gas porosity.[161] This approach may reduce porosity and heat treat the part in a single step, resulting in improved mechanical properties. HIP has been shown to be an effective method for improving the fatigue performance of additively produced alloy samples by closing and minimizing the internal pores,[162] however, there is still an absence of study and research on ceramic HIP that has to be developed. Most of these recent findings indicate that porosity in ceramics during the laser ceramic interaction in the LPBF process is primarily caused by factors such as incomplete melting, material evaporation, spattering, and unstable melt pool dynamics. Localized evaporation of elements, as well as keyhole formation and gas entrapment during the laser process, are significant contributors

to pore development. To control or minimize porosity and improve the quality of ceramic components, there is a clear need for optimizing laser parameters, a suitable atmosphere for experiments, enhancing material feedstock characteristics, and developing advanced monitoring techniques. Addressing these challenges will be important for advancing the industrial application of ceramic AM, particularly in achieving defect-free, high-strength components by LPBF.

Spattering effect is another major cause of keyhole porosity and an undesirable phenomenon influencing the layer levelness, surface morphology, overall density, and mechanical properties of the final part.[163] In addition, gaps, fractures, inclusions, and porosities may develop due to the solidification of spatters within the affected regions. The spattering effect is mainly produced by the splashed powder particles and molten droplets in the form of liquid spatters. Therefore, controlling the formation spatters and balling is an important task for reducing the porosity and associated defects. Ullah et al.[128] observed that the spattering behavior of ceramics differs slightly from that of metals and alloys due to variations in melting behavior and material properties. Ceramics exhibit a relatively low ratio of hot ejections because of their high melting points and poor thermal conductivity. However, partially heated ejected particles tend to adhere together and settle back on the layer's surface, potentially creating a spattering effect and becoming embedded in the final part. On the other side, when the laser energy input is too high, it results in vaporization and hot ejected particles in the form of vapor plumes that resolidify and produce spatters or balls after falling back into the molten pool. A slight variation in laser power and scanning speed varies the laser energy, which significantly influences the spattering effect. A summary of the key studies on the formation causes and prevention strategies of pores in ceramic LPBF processes is provided in Table 4. Besides the above mentioned parameters, laser beam shaping emerged as a hot topic in LPBF of metals[164,165] where the ring shape and top-hat beam profiles have shown significant effect on the controlling of spattering and porosity, which is expected to be a productive approach in ceramics manufacturing as well to control the above-mentioned flaws.

Dendrites and columnar grains

In the LPBF process for ceramics, dendrites, and columnar grains are microstructural features that arise due to the complex interplay between thermal gradients, solidification rates, and material properties.[3] Dendrites typically form in the rapidly solidified regions of the molten pool during LPBF. As the ceramic material melts and then quickly solidifies, the rapid cooling rates, coupled with steep thermal gradients, lead to the growth of dendritic structures. These structures are characterized by their tree-like morphology, consisting of a primary trunk with secondary and tertiary branches. Dendritic structures can significantly influence the mechanical properties of the printed part.[71] They tend to introduce anisotropy, meaning that the material's mechanical strength, fracture toughness, and other characteristics vary depending on the direction of the applied load relative to the dendritic orientation. Zhang et al.[91] investigates the morphology and formation mechanism of cracks in Al_2O_3–ZrO_2 eutectic ceramics fabricated via LPBF. In terms of columnar grains, ceramics exhibit multiple microstructural types, including eutectic, cellular, and dendritic structures. The columnar grains play a role in the crack propagation behavior, especially within the dendritic and eutectic regions, where anisotropy makes cracks more likely to propagate. The study observes that cracks are less likely to propagate in regions with cellular structures compared with those with columnar grains, as the cellular structures exhibit better crack inhibition through deflection and pinning effects. The growth of dendrites can be influenced by several laser processing parameters, such as power, scanning speed, and hatch spacing. Higher laser power creates a deeper molten pool, which promotes dendritic growth as the material solidifies. Conversely, lower laser power or higher scanning speeds can reduce the extent of dendrite formation. However, controlling dendritic structures is critical for optimizing the mechanical properties of ceramics produced via LPBF. Excessive dendritic growth may lead to defects such as microcracks, compromising mechanical performance. On the other hand, fine dendritic structures can enhance the hardness and strength of the ceramic part by impeding dislocation movement, providing some advantages in certain applications.[71,168]

Columnar grains, another microstructural feature in LPBF ceramics grow perpendicular to the solidification front, usually aligning with the direction of heat flow. These elongated grains form due to the directional cooling of the molten pool. In the LPBF process, columnar grains typically grow parallel to the movement of the laser, creating continuous grain structures that span multiple layers. The presence of columnar grains affects the mechanical anisotropy of the printed part, with different properties exhibited when the material is stressed parallel or perpendicular to the grain orientation. High cooling rates and steep thermal gradients favor the formation of fine columnar grains, while slower cooling rates result in coarser grains.[158] Recent research aims to manipulate grain structures by adjusting laser scanning patterns and layer thickness or employing preheating strategies to control grain growth. In a study,[162] the authors explore how supertransus HIP transforms the coarse columnar β-grains in Ti-22V-4Al into more refined equiaxed grains through

TABLE 4 Recent studies on the formation causes and prevention strategies of pores in ceramic LPBF processes.

References	Materials	Major findings
Pfeiffer et al.[144]	ZrW_2O_8 and $Al_2W_3O_{12}$	• Porosity was caused by material evaporation and process instabilities, with vacuum infiltration improving mechanical properties without reducing porosity. • Parameters optimization and process control is required.
Yao et al.[157]	Al_2O_3	• Porosity is caused by excessive keyhole depth and interface instability, requiring optimized energy density for defect-free tracks.
Wu et al.[166]	Si_3N_4	• Increasing AlN content in SLS-fabricated Si_3N_4 ceramics reduces porosity and enhances densification. • At 20 wt% AlN, total porosity decreases to 33.6%, while flexural strength increases to 23.9 MPa.
Liu et al.[154]	Al_2O_3–ZrO_2	• Porosity in ceramic laser AM is primarily influenced by remelting rate and overlap ratio, with key pore types being intracrystalline, interlayer, intralayer, and shrinkage pores.
Liu et al.[167]	Al_2O_3	• As sintering temperature increased, the porosity of Al_2O_3 PHM ceramic foams gradually decreased from 77.09 to 72.41%, while maintaining a uniform pore size distribution.
Ullah et al.[90]	TiO_2-Ti	• Increasing laser power and decreasing scanning speed reduced cracks, pores, and improved microstructure in TiO_2 L-PBF specimens • Enhancing columnar crystal formation and bonding reduced porosity
Rehman et al.[36]	Al_2O_3–MgO–SiC	• Lower MgO content and higher laser power improved surface quality and reduced defects in LPBF-fabricated Al_2O_3, with SiC being more effective than MgO in reducing surface defects.
Zhang et al.[168]	Al_2O_3	• Optimizing laser parameters can significantly reduce porosity in ceramic LPBF by improving energy absorption and melting efficiency. • Proper selection of powder properties and temperature control can minimize thermal stresses and further reduce porosity .
Ullah et al.[128]	Cu_2O	• Spattering and evaporation of materials is the key cause of high temp porosity. • Control of laser energy density plays significant role in porosity control.
Lei et al.[156]	Al_2O_3	• Increasing laser scanning speed reduced the permeation of molten Al_2O_3 into the surrounding porous paste, improving surface uniformity and reducing porosity in the laser-melted ceramic tracks.
Xiong et al.[118]	Al_2O_3–ZrO_2	• Laser defocus shift in LPBF impacts porosity and defect distribution. • Initial defocus reduces void defects and increases density. • Excessive defocus increases porosity and reduces surface quality.

dynamic recrystallization, particularly in regions where large pores collapse. This columnar-to-equiaxed transition improves the microstructure by reducing the size and texture of the remaining columnar grains, resulting in a more homogeneous grain morphology. The formation of strain-free equiaxed grains enhances the mechanical properties of the material, significantly increasing its ductility and strength. Although this study focuses on metals, the same principle applies to ceramics, where HIP and similar processes can refine grain structure, improve porosity, and enhance mechanical properties. These approaches allow for better control over the mechanical properties, reducing anisotropy and enhancing the overall performance of LPBF-fabricated ceramic parts.

Surface roughness

Surface roughness in LPBF-fabricated ceramics is a challenge that affects both the mechanical and functional properties of the printed components.[169] The layer-by-layer nature of the LPBF process, combined with the use of fine ceramic powders, inherently leads to surface irregularities. These irregularities arise from several factors, including powder particle size, layer thickness, laser parameters, and molten pool dynamics during solidification. The size and morphology of ceramic powder particles significantly influence surface roughness.[24,170] Coarser powders often lead to a rougher surface finish due to larger interstitial spaces between particles, which may not fully melt during the laser scanning process. Finer powders can achieve a smoother surface finish because they pack more densely and melt more uniformly. However, finer powders are more prone to issues like agglomeration and poor flowability, which can negatively affect layer deposition. The choice of layer thickness is another critical factor influencing surface finish; thinner layers generally result in finer surface roughness as the laser can

more precisely melt each layer, reducing the formation of ridges between layers. Laser processing parameters such as power, scanning speed, and hatch spacing directly affect surface quality.[169] Higher laser power can promote more uniform melting and smoother surfaces, but excessive power may result in spattering or balling, where molten material forms spherical droplets that solidify on the surface, increasing roughness. Insufficient laser power, on the other hand, can lead to incomplete melting and a rough surface characterized by partially fused particles. Careful optimization of laser scanning speed and hatch spacing is essential for achieving a smooth surface finish by allowing uniform melting and solidification across the build area.

To address surface roughness, several postprocessing techniques are commonly employed.[24] Mechanical polishing is effective for achieving a smooth finish but may be limited by the complexity of the part geometry. Chemical etching can selectively remove surface asperities without requiring physical contact, making it suitable for intricate shapes. Thermal postprocessing, such as sintering, can also reduce surface roughness by promoting grain growth and densification, which smooths surface irregularities. Furthermore, reducing layer thickness, optimizing laser power and scanning patterns, or using finer powder feedstock can directly enhance surface finish during the LPBF process itself.[27,171] By integrating these strategies, manufacturers can produce ceramic components with controlled surface roughness, meeting the stringent requirements of advanced engineering applications.

2.1.4 | Mechanical and physical properties of ceramic AM parts

Recently, ceramic AM has gained increasing interest in various industries due to its combination of imperative properties, making it suitable for a wide range of applications such as aerospace, healthcare, electronics, and energy.[172–174] The mechanical behavior of ceramic AM parts is a critical aspect that determines their suitability for various applications.[149] Ceramic materials are known for their excellent high-temperature resistance, chemical inertness, and electrical insulating properties.[172] Understanding the mechanical and physical properties of these parts is crucial for optimizing their performance and ensuring their suitability for specific applications. Some of the common ceramic materials used in the recent literature in terms of mechanical properties are shown in Table 5. Wikes et al. printed Al_2O_3–ZrO_2 ceramic structures by LPBF and printed ceramic parts with almost 100% densities. Preheating above 1600 degrees was provided to prevent the possible crack formation during the build process. Parts with fine-grained microstructures exhibit a flexural strength of above 500 MPa. Similarly, Verga et al.[72] printed alumina toughened zirconia by LPBF process and investigated part densities and mechanical properties. It was observed in their experiments that thermal postprocessing increased the density using dilatometry. Mechanical properties of the printed parts were checked by a four-point bending test after a posttreatment of 1300°C for 10 h in air. The maximum flexural strength was noted to be 31 ± 11 MPa as shown in Figure 12. The prepared samples could not withstand the load and were unsuccessful.

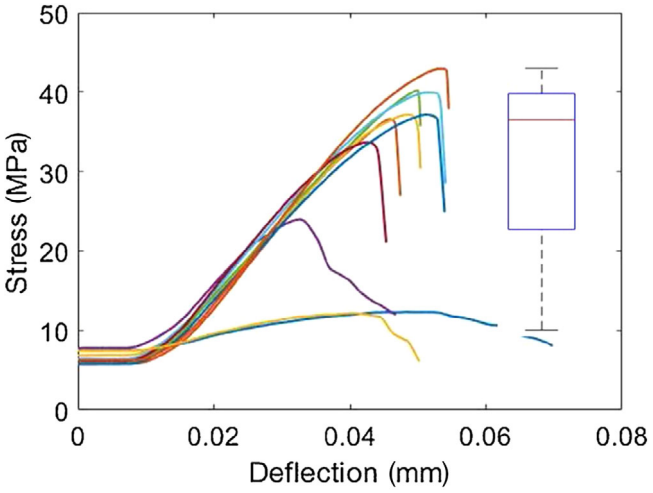

FIGURE 12 Flexural stress deflection curve for 10 measurements along with a box plot showing median and standard deviation. (Reproduced with permission from Ref. 72, Copyright 2020, Elsevier.)

Various approaches have been used in the literature to tailor the microstructure of printed ceramics by varying and optimizing the process parameters to achieve maximum mechanical properties. Xiong et al.[84] studied the effect of scanning speed on mechanical properties and microstructure evolution of Al_2O_3–ZrO_2 eutectic ceramics. Scanning speed optimization is pivotal in defining LPBF ceramic printing quality, while microstructure fine-tuning enhances toughness, reducing defects and boosting part performance. The authors found in their experiments that the hardness of printed ceramics first increased with scanning speed (60–120 mm/s) and then decreased with further increasing speed up to 200 mm/s. The maximum value of hardness was found to be 16.7 GPa at 120 mm/s. The increase in scanning speed up to 120 mm/s resulted in a fine microstructure, which enhanced the hardness of the ceramics. However, beyond 120 mm/s, LOF and other defects contributed to the poor hardness, as shown in Figures 13 and 14. For low or even no defects and improved mechanical properties, optimization of the process parameters, especially the scanning speed, helps us to improve the experimental design. Jue et al.[176] studied the

TABLE 5 Different ceramics and their corresponding enhanced mechanical properties quantitatively.

Feedstock	Technology	Printing parameters	Density	Mechanical properties	References
Al–Al_2O_3	LPBF	• Scanning speed: 300 mm/s • Energy density: 317.5 J/mm^3	99.49	• Maximum hardness achieved 48.35 HV0.1 • Yield strength 109 MPa • Ultimate tensile strength 160 MPa • Increase in yield strength up to 36% • Increase in microhardness up to 17% • Increase in cold work sample hardness up to 39%	[175]
Al_2O_3–ZrO_2	Homemade ceramic LPBF	• Laser power: 100 W • Hatch distance: 100 μm • Spot dia: 100 μm • Layer thickness: 50 μm	Not studied	• Maximum hardness: 16.7 GPa • Maximum fracture toughness: 7.76 MPa $m^{1}/^{2}$	[84]
Al–Al_2O_3	LPBF	• Laser power 130 W • Spot size: 70 μm • Layer thickness: 70 μm • Scanning speed: 450, 550, 650, 750 mm/s	~97%	• Maximum hardness achieved: 175 HV0.1 • Coefficient of friction: 0.11 • Low wear rate achieved: 4.75×10^{-5} mm^3/N m	[176]
TiB_2/Al_2O_3–ZrO_2	LPBF	• Laser power: 100 W • Scanning speed: 100 mm/s • Thickness: 50 μm	Not studied	• Hardness: ~2000 HV (with 3 wt% TiB_2 • Fracture Toughness: 5.97 Mpa $m^{1}/^{2}$ • Surface roughness: 5.5 μm	[177]
$Al_2Si_4O_{10}$–Al	LPBF	• Laser power 140 W • Scanning speed 400, 500, 600, 700 mm/s	–	• Nanohardness achieved 3.79 GPa • Low coefficient of friction 0.32 • Wear rate 4.52 105 mm^3/N m	[178]
$RE_3Al_5O_{12}$	Ceramic-LPBF	• Laser power: 80 W • Scanning speed: 40–120 mm/s • Layer thickness: 50 μm	97.83 ± 0.55% (at 60 mm/s)	• Hardness: 15.09 ± 0.68 GPa (at 120 mm/s) • Grain size reduction from 44.39 to 12.52 μm with increased speed	[64]
$Al_2O_3/GdAlO_3$	Homemade printer	• Layer thickness 0.5 mm • Overlap ratio 50% • Laser power: 100–450 W	>95%	• Maximum hardness achieved 17 GPa • Maximum fracture toughness obtained 4.5 MPa/m^2	[179]
Ti_2AlC	Homemade printer	• Layer thickness: 0.5 mm • Scanning spacing 50 μm	70–80%	Maximum compressive strength obtained 30 MPa	[180]

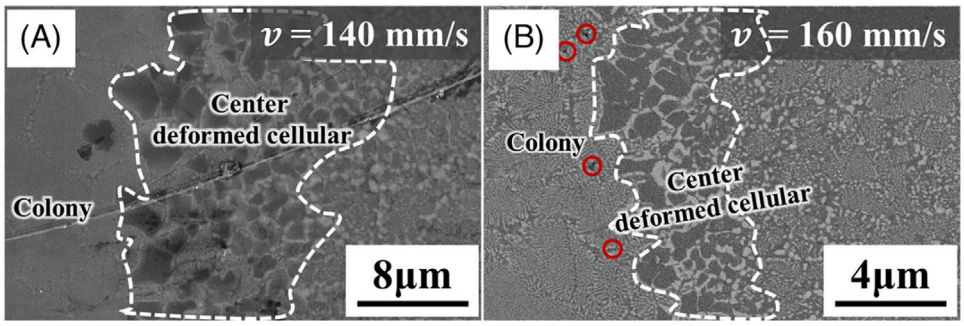

FIGURE 13 SEM schematic diagram of the microstructures of samples prepared by LPBF under different laser scanning speeds: (A) 140 mm/s and (B) 160 mm/s. (Reproduced with permission from Ref. 84, Copyright Wiley 2023.)

influence of LPBF processing parameters on densification, microstructure, hardness and wear resistance in detail. A wide range of scanning speed from 450 to 750 mm/s was used. According to their results, a fully dense part with theoretical density of 97% was achieved when the 550 mm/s scanning speed was applied. However, with the decrease of scanning speed, there was a direct effect on the microstructure and showed a significant coarse morphology. The fully dense parts had excellent hardness with a maximum value of 175 HV0.1 and a low coefficient of friction of 0.11. Overall, the defects inside the parts and mechanical properties were considerably improved when a scanning speed of 550 mm/s was employed.[176] In another study by the authors, they varied the scanning speed from 400 to 700

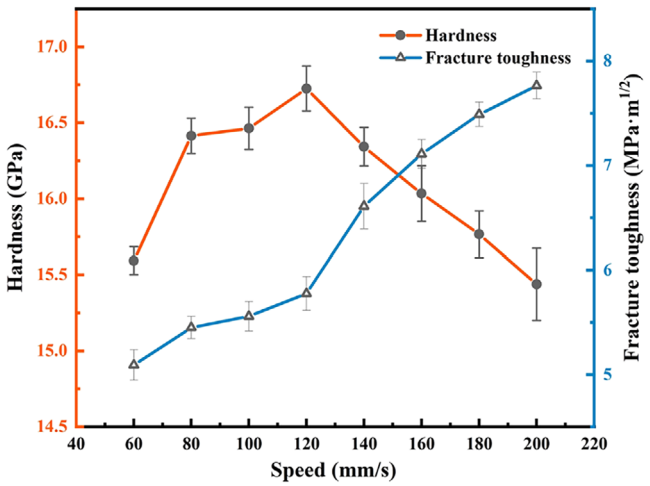

FIGURE 14 Vickers hardness and fracture toughness on the upper surface of the sample under different LPBF scanning speeds. (Reproduced with permission from Ref. 84, Copyright Wiley 2023.)

with 100 differences. The scanning speed of 500 mm/s was found to be an optimal speed, and the printed parts exhibited excellent wear performance with a considerably low coefficient of friction[178].

Shen et al.[179] examined the same scanning strategy and investigated the macromorphology, microstructure evolution, rapid solidification behavior, and mechanical properties of the printed ceramics at different processing parameters. As previously mentioned, the scanning speed affects the microstructure and corresponding mechanical properties. Here, by increasing the scanning speed, the microstructure to complex regular eutectic from fine irregular eutectics. It is obvious from their experiments that when making ceramics using LPBF, gradually heating the base material before adding ceramic layers reduces stress between them, leading to better-quality ceramic parts. The microhardness of the printed ceramics was found to be 17 GPa and fracture toughness of 4.5 MPa/m^2. Postprocessing also enhances the microstructure and thus improves the mechanical properties of the resulting printed parts. Han et al.[175] used Al–Al_2O_3 composites and studied the effect of cold working on microstructure and mechanical properties in detail.[175] Also, a finite element model was developed in order to predict the thermal behavior in detail. According to their results, the optimum scanning speed was 300 mm/s, and the ED of 317 J/mm^3 in order to print fully dense parts of about 99%. Investigations of microstructure revealed that the as printed specimens had a fine granular microstructure because of rapid cooling. The addition of alumina impacted the mechanical properties very much as the yield strength was increased up to 36% and microhardness up to 17%. The parts undergoing cold work samples increased the microhardness up to 39% as Figure 15. This was due to the plastic deformation that resulted in grain elongation.

Different processing can be altered to manage and optimize the mechanical properties and microstructure in detail. Li et al.[180] printed Ti_2AlC MAX-phase ceramic matrix composites and investigated the microstructure evolution and mechanical properties of the printed ceramics under different Nb contents and sintering temperatures. The Nb content and sintering temperatures can significantly affect the microstructure of printed samples. As the sintering temperature was raised from 1200 to 1400°C, the width of a specific structure in the material called Ti_2AlC increased from being very thin (0.36 μm) to much wider (1.58 μm). Similarly, the compressive strength ranges from 17.5 to 30.3 MPa for the ceramic samples. The best compressive strength of 30.3 MPa was achieved when a small amount of another material (1 wt% of Nb) was added and the sintering temperature was set at 1300°C. So, by adjusting the temperature and adding a bit of another substance, they were able to make the ceramic material very strong.

Considering that LPBF of ceramic is still at early stage of research, poor mechanical properties of ceramics parts printed by LPBF processes are of concern and topic of research nowadays.[172,27] Efforts to enhance the mechanical properties of ceramic parts involve meticulous parameter optimization, including layer thickness, laser power, and scanning speed, to control sintering and minimize defects. Advanced material selection, postprocessing techniques like HIP, and innovative monitoring methods are also being explored to mitigate challenges associated with ceramic brittleness and achieve superior mechanical performance in LPBF-printed ceramics, opening up opportunities for their utilization in demanding engineering applications. Overall, the mechanical properties of ceramics pose unique challenges in AM techniques, especially the laser-based process. Ceramics are generally harder, and more brittle compared with metals and polymers, making them susceptible to cracking during the printing process and during the postprocessing. Moreover, their mechanical behavior can vary significantly under different conditions and cannot be predicted. To harness the full potential of ceramics in LPBF, extensive research and development efforts are required to fine-tune printing parameters, explore new materials, and gain a deeper understanding of how to enhance their mechanical properties.

2.2 | Computational modeling and simulation in ceramic AM

The temperature field varies quickly during the LPBF process, making it challenging to obtain the dynamic

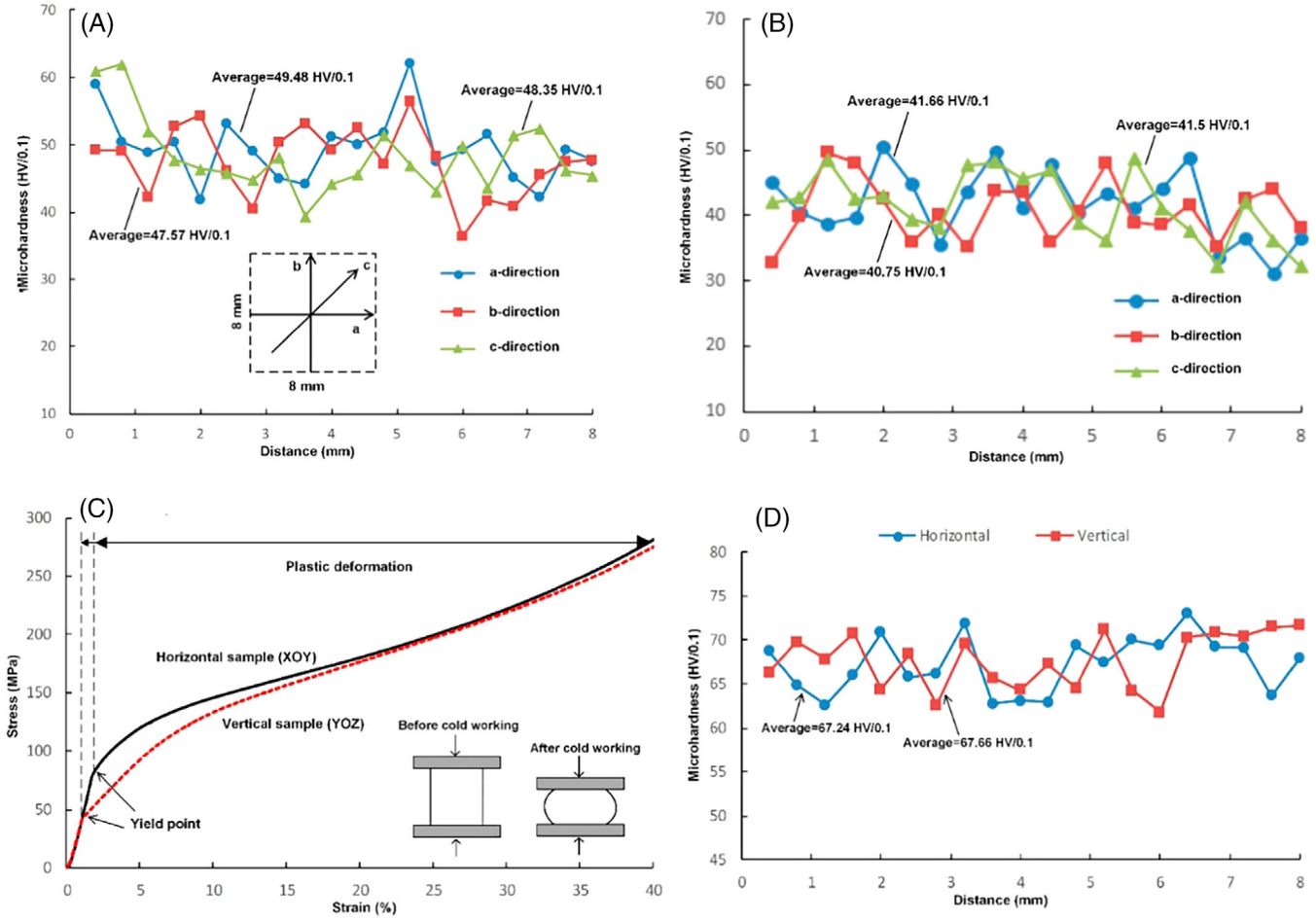

FIGURE 15 Microhardness of the samples fabricated at 300 mm/s: (A) composite and (B) pure Al; (C) stress–strain curve of the composite samples under cold working; (D) microhardness of the samples subjected to cold working. (Reproduced with permission from Ref. 181, Copyright, Elsevier 2017.)

temperature field and variation pattern using the experimental approach. As a result, numerical modelling techniques have become important for depicting the LPBF process's dynamic temperature field. For instance, a temperature field and thermal stress distributions are studied for $Al_2O_3/GdAlO_3/ZrO_2$ ternary eutectic ceramics using the LPBF method with the aid of a finite element method (FEM) to explore an optimized process and creatively disclose the crack formation mechanism and propagation behavior via a single track, a single layer, and multilayers.[182] Figure 16 shows the summary of the FEM simulation in detail.

Another numerical model for transient thermal analysis based on the FEM was developed to represent the dynamic temperature field during the process of LPBF of nano-hydroxyapatite ceramic powder.[183] A comparison study between experimental and numerical simulation using the LPBF process is reported for alumina ceramic.[184] A developed numerical model has been used to predict and choose the process parameters, and the alumina powder has been adapted and modified to be used for the LPBF process using the spray-drying technique. The other parameters have been predicted numerically, and various scanning speeds of 100, 200, 300, and 400 mm/s have been taken into consideration as shown in Figure 17.

Similarly, a level set FEM is used to model the LPBF process that is applied to alumina ceramic at the bead formation scale.[185] They examined how surface tension and liquid viscosity affect melt pool dynamics. Additionally, they use three-dimensional simulations of multiple passes to examine the impact of the scanning strategy. They have extended this study by considering the effects of surface tension and the Marangoni force in the analysis.[186] Luo et al.[187] developed a three-dimensional nonlinear transient finite element model to study the temperature and stress fields during the LPBF processing of a single tin telluride ceramic layer. They have considered a volume heat source to study the local absorption of the

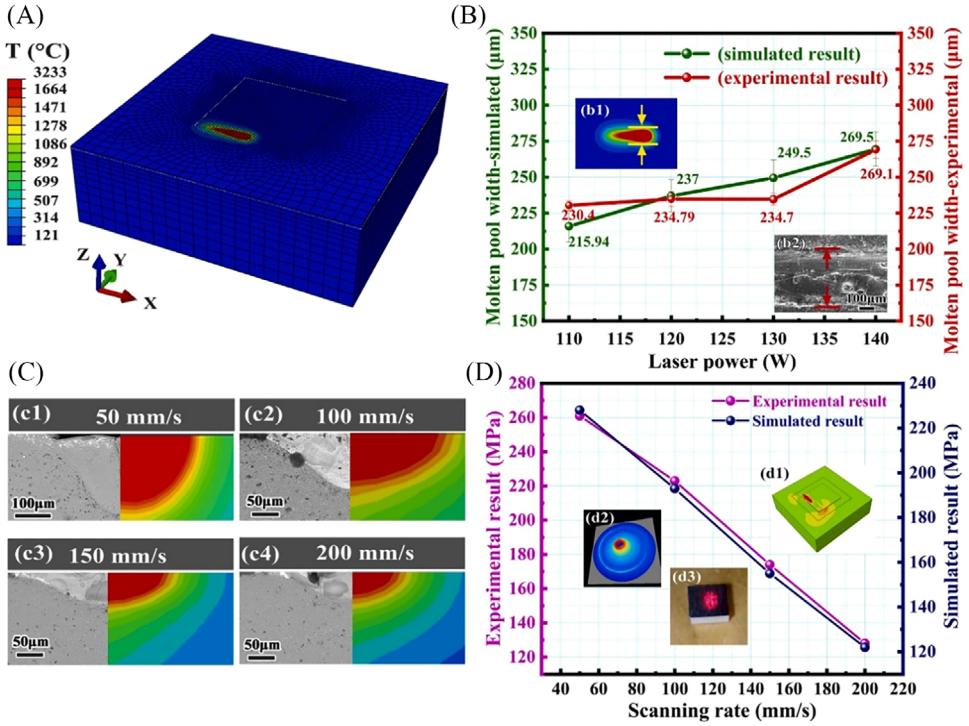

FIGURE 16 FEM simulation validated by experimental results: (A) single-layer FEM model and molten pool profile. (B) Simulation results: (B1) molten pool width validated experimentally, (B2) profiles at varying laser powers. (C) Molten pool morphology from FEM and single-track experiments at different scanning rates (C1–C4: 50–200 mm/s, 150 W). (D) Residual stress simulation: (D1) FEM prediction and (D2–D3) validation via XRD Debye ring tests.[182]

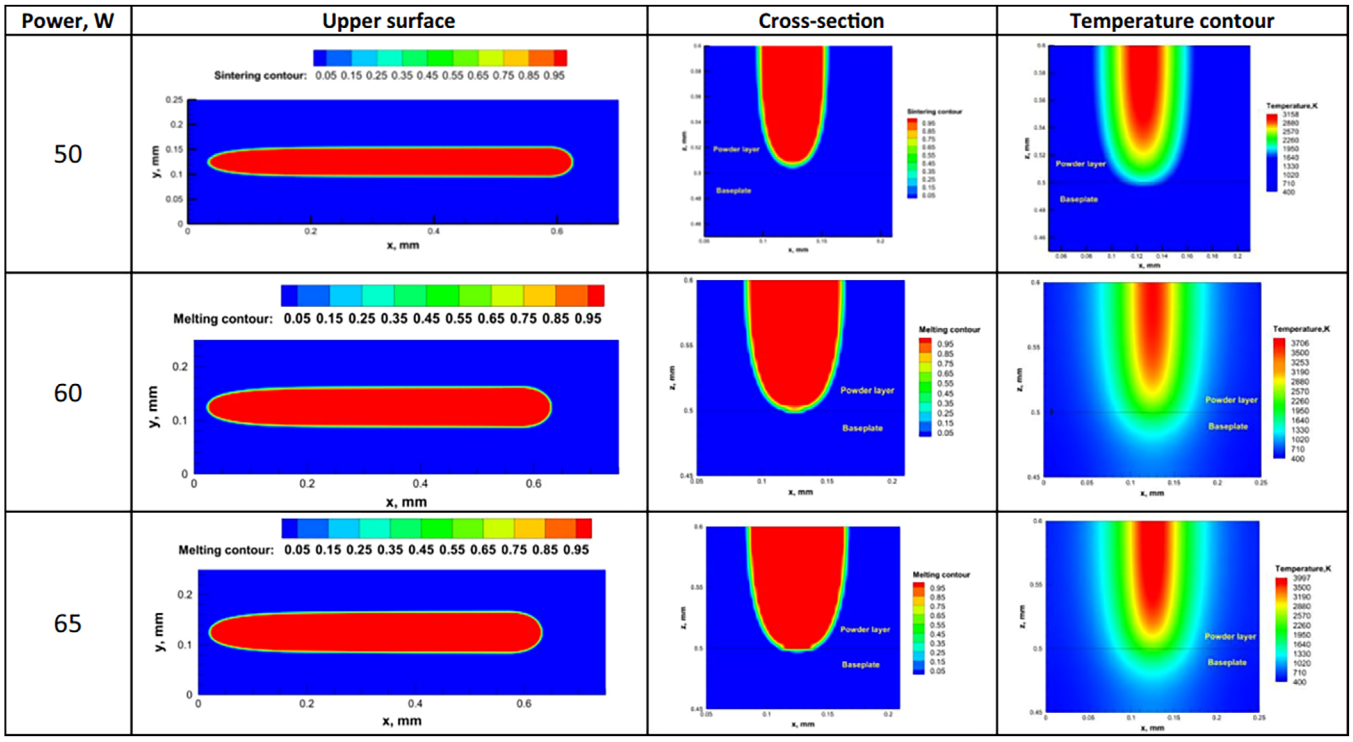

FIGURE 17 Melting contour and temperature distribution at changed positions for a scanning speed of 100 mm/s.[184]

TABLE 6 Summary of simulation studies utilizing various numerical methods to analyze the LPBF process for ceramic materials.

Numerical method	Analysis	Ceramic material	Dimension	Heat source	References
Finite element method	Transient heat transfer analysis	Glass	3D	Gaussian	[189]
	Thermo-fluid	Silicon carbide	3D	Gaussian	[190]
	Thermo-mechanical	TiB_2/Al–Si	2D	N/A	[191]
	Thermo-fluid	$TiAl_6V_4$	3D	Gaussian	[192]
	Transient thermo-mechanical	Nano-hydroxyapatite	3D	Gaussian	[183]
	Transient thermo-mechanical	Alumina	3D	Volume heat source based on Beer-Lamber law	[185, 186]
	Nonlinear transient thermo-mechanical	Tin telluride (SnTe)	3D	Gaussian	[187]
	Thermal fluid	Alumina	2D	Gaussian	[188]

laser-transparent material. A comparison study between simulations and experiments for a single-track has been undertaken for the LPBF of alumina with Yb: YAG laser.[188] They have used high scanning speeds to investigate cases of the balling effect. Recently, glass has been additively manufactured using LPBF, showing promise for use in small-scale applications like flow reactors for the chemical engineering and pharmaceutical manufacturing sectors. The impact of processing parameters and the thermal response of the laser-glass powder bed interaction is examined in a recent study using a transient heat transfer finite element analysis.[189] Table 6 summarizes simulation studies on the LPBF process for ceramics, highlighting methods, materials, dimensions, heat sources, and references.

2.3 | Challenges and outlook in LPBF of ceramics

Despite the significant advancements in AM of ceramics, this field continues to face numerous challenges that hinder its widespread industrial adoption. The inherent properties of ceramics such as their high melting points, brittleness, and poor thermal shock resistance present significant difficulties when applied to AM processes. However, alongside these challenges, ongoing research and innovation are opening promising avenues to overcome these obstacles and enhance the overall feasibility of ceramic AM for industrial applications. The following sections provide an in-depth exploration of the key challenges and limitations currently facing ceramic AM, as well as potential future directions aimed at addressing these issues. By focusing on process optimization, material development, and advanced manufacturing techniques, the future of ceramic AM holds significant potential for broader industrial adoption and application.

2.3.1 | Key challenges and limitations

1. One of the most critical challenges lies in managing crack formation and residual stresses during processing. Ceramics are prone to cracking due to the rapid thermal cycles involved in processes like LPBF and direct energy deposition (DED). These rapid heating and cooling cycles induce significant temperature gradients, leading to the development of tensile stresses that the brittle ceramic material cannot withstand. Cracks that form during the solidification of the molten pool severely compromise the mechanical integrity of the part, often resulting in reduced strength and early failure under operational conditions. Even slight adjustments in laser power, scan speed, or hatch spacing may not eliminate these defects, indicating the need for more sophisticated control of process parameters and thermal management.
2. Porosity is another significant issue in the AM of ceramics. Spherical gas pores and irregular pores caused by incomplete fusion are commonly observed in ceramics processed via LPBF and DED. These pores not only reduce the material's density but also act as stress concentrators that exacerbate crack propagation. While increasing the energy input from the laser or electron beam can help in reducing porosity, excessive energy can lead to material evaporation, spattering, and the formation of other surface defects like roughness and balling. The balance between avoiding porosity and controlling the energy input remains a delicate one that has yet to be fully optimized.
3. Effective laser–material interaction is critical for efficient energy transfer during LPBF. However, most ceramics exhibit low laser absorptance, especially in their natural state. This means that the ceramic powders do not absorb enough laser energy, leading to incomplete melting and material defects. Dopants like

magnesium oxide (MgO) and silicon carbide (SiC) are being explored to improve the absorptance and alter the thermal properties of the ceramic powder. Furthermore, laser power and scan speed directly impact the amount of heat transferred to the ceramic powder, influencing melt pool dynamics. Achieving the right balance between these parameters is crucial but challenging, especially for larger parts where different regions experience varying thermal conditions.

4. Material feedstock quality is also a major factor contributing to defects. The use of irregularly shaped or inconsistently sized powder particles can result in poor layer deposition, leading to uneven melting, void formation, and surface defects. This issue is further complicated by the fact that ceramic powders tend to have poorer flowability compared with metal powders, making it difficult to form uniform layers during the powder spreading stage of LPBF or BJ. Developing high-quality, spherical ceramic powders with better flowability and packing characteristics remains an area requiring further research.
5. In addition to material-related challenges, the high costs and limited availability of equipment suitable for ceramic AM are significant barriers to widespread use. For instance, the specialized laser and electron beam systems required to handle ceramics with high melting points are expensive and not as widely available as their metal or polymer counterparts. Furthermore, many of the existing AM machines are designed primarily for metals or polymers and require significant modifications to process ceramics efficiently. For example, improving the preheating systems or modifying the beam profiles to distribute energy more uniformly is often necessary but adds complexity and cost to the process.
6. Postprocessing requirements, such as sintering and HIP, are also a challenge. Many ceramic components fabricated via AM require additional postprocessing to eliminate defects like porosity and improve mechanical properties. These postprocessing steps add time, cost, and complexity to the overall production cycle. Moreover, the sintering process itself can introduce challenges such as shrinkage and warping, which further complicate the fabrication of high-precision parts.
7. Scalability remains a significant hurdle. While AM has shown promise in producing small, intricate ceramic components, scaling these processes to produce larger parts with consistent quality is a challenge. The larger the part, the more difficult it becomes to manage thermal gradients and avoid defects like cracks, porosity, and warping. Moreover, the build times for large components are considerably longer, which limits the practicality of AM for mass production in its current form.

2.3.2 | Opportunities and future perspectives

Despite the challenges faced in LPBF of ceramics, ongoing research and technological advancements offer promising solutions that can significantly improve the efficiency and viability of ceramic AM.

1. One of the most important areas of future development is process optimization through advanced computational modeling and simulation. As highlighted in this review, numerical simulations of thermal gradients, residual stresses, and material behavior can help identify optimal process parameters and reduce the trial-and-error approach currently prevalent in ceramic AM. These simulations will become more accurate and predictive as computational power increases and more experimental data are integrated into the models.
2. The development of advanced materials tailored specifically for AM processes is another critical area for future research. Innovations in powder production, such as the development of ceramic powders with optimized particle size distributions and improved flowability, could dramatically improve the quality of the parts produced. The introduction of reinforcement phases, such as ZrO_2 or SiC, has already shown promise in improving the toughness of ceramic parts and reducing defects like cracking. Future research may focus on creating novel ceramic composites that are better suited to withstand the high thermal stresses of AM processes.
3. Another potential solution to some of the current challenges is the integration of in situ monitoring and feedback control systems. By implementing real-time monitoring systems that can detect defects like cracks, porosity, or uneven layer deposition during the printing process, it may be possible to adjust process parameters on the fly and prevent defects before they become critical. For example, high-resolution thermal cameras or laser-based sensors could be used to monitor the temperature distribution in the part and adjust laser power or scan speed accordingly to avoid excessive thermal gradients.
4. Laser beam shaping is also a promising research direction. Moving beyond traditional Gaussian laser profiles, alternative beam shapes like top-hat or donut profiles could distribute the energy more evenly across the powder bed, reducing thermal stresses and improving part quality. This approach has shown success in metal AM and holds potential for ceramics as well.

5. Postprocessing advancements will also be crucial for realizing the full potential of ceramic AM. Techniques like HIP, annealing, and advanced sintering methods can help to close pores, eliminate cracks, and improve the mechanical properties of printed parts. However, these processes need to be further optimized and integrated more seamlessly into the overall manufacturing workflow to reduce costs and processing times.
6. Finally, collaboration between academia, industry, and government will be key to accelerating the development and adoption of ceramic AM technologies. Large-scale initiatives aimed at standardizing processes, developing new materials, and sharing research findings could help overcome the current barriers. The potential for ceramic AM to revolutionize industries like aerospace, healthcare, and electronics is immense, but realizing this potential will require concerted efforts from all stakeholders.

ACKNOWLEDGMENTS

This work was supported by a fellowship of the German Academic Exchange Service (DAAD). This project has also received funding from the European Union's Horizon 2020 Research and Innovation Program under the Marie Skłodowska-Curie Grant Agreement No. 101034328. This paper reflects only the author's view and the Research Executive Agency, and the European Commission are not responsible for any use that may be made of the information it contains.

ORCID

Abid Ullah https://orcid.org/0000-0002-8692-8592
Zulfiqar Ali https://orcid.org/0000-0001-9641-3165

REFERENCES

1. Ayode Otitoju T, Ugochukwu Okoye P, Chen G, Li Y, Onyeka Okoye M, Li S. Advanced ceramic components: materials, fabrication, and applications. J Ind Eng Chem. 2020;85:34–65. https://doi.org/10.1016/j.jiec.2020.02.002
2. Hasirci V, Hasirci N. Ceramics. In: Hasirci V, Hasirci N (eds.) Fundamentals of biomaterials. Cham: Springer International Publishing; 2024. p. 57–70
3. Dadkhah M, Tulliani J-M, Saboori A, Iuliano L. Additive manufacturing of ceramics: advances, challenges, and outlook. J Eur Ceram Soc. 2023;43:6635–64. https://doi.org/10.1016/j.jeurceramsoc.2023.07.033
4. Belmonte M. Advanced ceramic materials for high temperature applications. Adv Eng Mater. 2006;8:693–703. https://doi.org/10.1002/adem.200500269
5. Sharma A, Babbar A, Tian Y, Pathri BP, Gupta M, Singh R. Machining of ceramic materials: a state-of-the-art review. International Journal on Interactive Design and Manufacturing (IJIDeM). 2023;17:2891–911. https://doi.org/10.1007/s12008-022-01016-7
6. Li X, Guo Z, Huang Q, Yuan C. Research and application of biomimetic modified ceramics and ceramic composites: a review. J Am Ceram Soc. 2024;107:663–97. https://doi.org/10.1111/jace.19490
7. Randall Curlee T, Das S. Advanced materials: information and analysis needs. Resour Policy. 1991;17:316–31. https://doi.org/10.1016/0301-4207(91)90016-O
8. Ribeiro MJ, Tulyaganov D. Traditional ceramics manufacturing. In: Baino F, Tomalino M, Tulyaganov D (eds.) Ceramics, glass and glass-ceramics: from early manufacturing steps towards modern frontiers. Cham: Springer International Publishing; 2021. p. 75–118
9. Prakash C, Singh S, Kopperi H, Ramakrihna S, Mohan SV. Comparative job production based life cycle assessment of conventional and additive manufacturing assisted investment casting of aluminium: a case study. J Clean Prod. 2021;289:125164. https://doi.org/10.1016/j.jclepro.2020.125164
10. Nazari K, Tran P, Tan P, Ghazlan A, Ngo TD, Xie YM. Advanced manufacturing methods for ceramic and bioinspired ceramic composites: a review. Open Ceramics. 2023;15:100399. https://doi.org/10.1016/j.oceram.2023.100399
11. Diao Q, Zeng Y, Chen J. The applications and latest progress of ceramic 3D printing. Additive Manufacturing Frontiers. 2024;3:200113. https://doi.org/10.1016/j.amf.2024.200113
12. Lakhdar Y, Tuck C, Binner J, Terry A, Goodridge R. Additive manufacturing of advanced ceramic materials. Prog Mater Sci. 2021;116:100736. https://doi.org/10.1016/j.pmatsci.2020.100736
13. Yves-Christian H, Jan W, Wilhelm M, Konrad W, Reinhart P. Net shaped high performance oxide ceramic parts by selective laser melting. Phys Procedia. 2010;5:587–94. https://doi.org/10.1016/j.phpro.2010.08.086
14. Srivastava M, Rathee S, Maheshwari S, Kundra TK. Comparison of additive manufacturing with conventional manufacturing processes. Presented at the September 17. 2019.
15. Chua C, Liu Y, Williams RJ, Chua CK, Sing SL. In-process and post-process strategies for part quality assessment in metal powder bed fusion: a review. J Manuf Syst. 2024;73:75–105. https://doi.org/10.1016/j.jmsy.2024.01.004
16. Wohlers Associates: Wohlers Report 2024. 2024. https://www.3dnatives.com/en/wohlers-report-2024-growth-of-metal-additive-manufacturing-040420245/
17. Sing SL, Yeong WY, Wiria FE, Tay BY, Zhao Z, Zhao L, et al. Direct selective laser sintering and melting of ceramics: a review. Rapid Prototyp J. 2017;23:611–23. https://doi.org/10.1108/RPJ-11-2015-0178
18. Narasimharaju SR, Zeng W, See TL, Zhu Z, Scott P, Jiang X, et al: A comprehensive review on laser powder bed fusion of steels: processing, microstructure, defects and control methods, mechanical properties, current challenges and future trends. J Manuf Process. 2022;75:375–414. https://doi.org/10.1016/j.jmapro.2021.12.033
19. Lüddecke A, Pannitz O, Zetzener H, Sehrt JT, Kwade A. Powder properties and flowability measurements of tailored nanocomposites for powder bed fusion applications. Mater Des. 2021;202:109536. https://doi.org/10.1016/j.matdes.2021.109536
20. Berger C, Schimo-Aichhorn G, Gronau S, Saft F, Seiringer S, Scheithauer U. Potential and challenges for powder bed fusion—laser beam (PBF-LB) in industrial ceramic additive

manufacturing. Open Ceramics. 2024;18:100614. https://doi.org/10.1016/j.oceram.2024.100614
21. Nabavi SF, Dalir H, Farshidianfar A. A comprehensive review of recent advances in laser powder bed fusion characteristics modeling: metallurgical and defects. Int J Adv Manuf Tech. 2024;132:2233–69. https://doi.org/10.1007/s00170-024-13491-1
22. Batool M, Abid MA, Javed T, Haider MN. Applications of biodegradable polymers and ceramics for bone regeneration: a mini-review. Int J Polym Mater Polym. Biomater. 1–15. https://doi.org/10.1080/00914037.2024.2314601
23. Makurat-Kasprolewicz B, Ipakchi H, Rajaee P, Ossowska A, Hejna A, Farokhi M, et al. Green engineered biomaterials for bone repair and regeneration: Printing technologies and fracture analysis. Chem Eng J. 2024;494:152703. https://doi.org/10.1016/j.cej.2024.152703
24. Mahajan A, Devgan S. Recent advances in surface engineering of additive manufactured materials for enhancing corrosion resistance. Progress in Additive Manufacturing. 2025;10:1103–18. https://doi.org/10.1007/s40964-024-00722-w
25. Chiari A, Mantovani S, Berzaghi A, Bellucci D, Bortolini S, Cannillo V. Load bearing capability of three-units 4Y-TZP monolithic fixed dental prostheses: An innovative model for reliable testing. Mater Des. 2023;227:111751. https://doi.org/10.1016/j.matdes.2023.111751
26. Zhou Q, Su X, Wu J, Zhang X, Su R, Ma L, et al: Additive manufacturing of bioceramic implants for restoration bone engineering: technologies, advances, and future perspectives. ACS Biomater Sci Eng. 2023;9:1164–89. https://doi.org/10.1021/acsbiomaterials.2c01164
27. Gopal PM, Kavimani V, Gupta K, Marinkovic D. Laser-based manufacturing of ceramics: a review. Micromachines (Basel). 2023;14:1564. https://doi.org/10.3390/mi14081564
28. Dubey D, Singh SP, Behera BK. Review: additive manufacturing of fiber-reinforced composites. J Mater Sci. 2024;59:12219–56. https://doi.org/10.1007/s10853-024-09925-6
29. Zhou S, Liu G, Wang C, Zhang Y, Yan C, Shi Y. Thermal debinding for stereolithography additive manufacturing of advanced ceramic parts: A comprehensive review. Mater Des. 2024;238:112632. https://doi.org/10.1016/j.matdes.2024.112632
30. Zeng Y, Wang J, Liu X, Xue Y, Tang L, Tong Y, et al: Laser additive manufacturing of ceramic reinforced titanium matrix composites: A review of microstructure, properties, auxiliary processes, and simulations. Compos Part A Appl Sci Manuf. 2024;177:107941. https://doi.org/10.1016/j.compositesa.2023.107941
31. Soni R, Verma R, Kumar Garg R, Singh H. Progress in aerospace materials and ablation resistant coatings: a focused review. Opt Laser Technol. 2024;177:111160. https://doi.org/10.1016/j.optlastec.2024.111160
32. Sun H, Zou B, Wang X, Chen W, Zhang G, Quan T, et al: Advancements in multi-material additive manufacturing of advanced ceramics: a review of strategies, techniques and equipment. Mater Chem Phys. 2024;319:129337. https://doi.org/10.1016/j.matchemphys.2024.129337
33. Wang J-C, Dommati H, Hsieh S-J. Review of additive manufacturing methods for high-performance ceramic materials. Int J Adv Manuf Tech. 2019;103:2627–47. https://doi.org/10.1007/s00170-019-03669-3
34. Ullah A, Ur Rehman A, Salamci MU, Pıtır F, Liu T. The influence of laser power and scanning speed on the microstructure and surface morphology of Cu2O parts in SLM. Rapid Prototyp J. 2022;28:1796–807. https://doi.org/10.1108/RPJ-12-2021-0342
35. Chen S, Shu X, Li Z, Wang D, Ren Z: Optimization of process parameters for LPBF forming TC11/SiC single track. MATEC Web Conf. 2024;401:2007. https://doi.org/10.1051/matecconf/202440102007
36. Ur Rehman A, Ullah A, Liu T, Ur Rehman R, Salamci MU. Additive manufacturing of Al2O3 ceramics with MgO/SiC contents by laser powder bed fusion process. Front Chem. 2023;11. https://doi.org/10.3389/fchem.2023.1034473
37. Keicher DM, Jellison JL, Schanwald LP, Romero JA, Abbott DH. Towards a reliable laser spray powder deposition system through process characterization. Presented at the. 1995.
38. Fan Z, Tan Q, Kang C, Huang H. Advances and challenges in direct additive manufacturing of dense ceramic oxides. 2024.
39. Rao H, Oleksak RP, Favara K, Harooni A, Dutta B, Maurice D. Behavior of yttria-stabilized zirconia (YSZ) during laser direct energy deposition of an Inconel 625-YSZ cermet. Addit Manuf. 2020;31:100932. https://doi.org/10.1016/j.addma.2019.100932
40. Snelling DA, Williams CB, Suchicital CTA, Druschitz AP. Binder jetting advanced ceramics for metal-ceramic composite structures. Int J Adv Manuf Tech. 2017;92:531–45. https://doi.org/10.1007/s00170-017-0139-y
41. Kunchala P, Kappagantula K. 3D printing high density ceramics using binder jetting with nanoparticle densifiers. Mater Des. 2018;155:443–50. https://doi.org/10.1016/j.matdes.2018.06.009
42. Lv X, Ye F, Cheng L, Fan S, Liu Y. Binder jetting of ceramics: Powders, binders, printing parameters, equipment, and post-treatment. Ceram Int. 2019;45:12609–24. https://doi.org/10.1016/j.ceramint.2019.04.012
43. Feilden E. Additive manufacturing of ceramics and ceramic composites via robocasting. 2017.
44. Janek M, Žilinská V, Kovár V, Hajdúchová Z, Tomanová K, Peciar P, et al: Mechanical testing of hydroxyapatite filaments for tissue scaffolds preparation by fused deposition of ceramics. J Eur Ceram Soc. 2020;40:4932–38. https://doi.org/10.1016/j.jeurceramsoc.2020.01.061
45. Chen X, Sun J, Guo B, Wang Y, Yu S, Wang W, et al: Effect of the particle size on the performance of BaTiO3 piezoelectric ceramics produced by additive manufacturing. Ceram Int. 2022;48:1285–92. https://doi.org/10.1016/j.ceramint.2021.09.213
46. Kim YJ, Kim HN, Kim DY. A study on effects of curing and machining conditions in post-processing of SLA additive manufactured polymer. J Manuf Process. 2024;119:511–19. https://doi.org/10.1016/j.jmapro.2024.03.112
47. Liu J, Zhu R, Zhang T, Wang X, Tang Y. Fabrication and properties of SiO2f/SiO2 composite ceramic based on stereolithography technology. J Asian Ceram Soc. 2024;12:141–50. https://doi.org/10.1080/21870764.2024.2324526
48. Lube T, Staudacher M, Hofer A-K, Schlacher J, Bermejo R. Stereolithographic 3D printing of ceramics: challenges and opportunities for structural integrity. Adv Eng Mater. 2023;25:2200520. https://doi.org/10.1002/adem.202200520
49. Weiss LE, Prinz FB. Novel applications and implementations of shape deposition manufacturing. Presented at the. 1998.

50. Weiss LE, Merz R, Prinz FB, Neplotnik G, Padmanabhan P, Schultz L, et al: Shape deposition manufacturing of heterogeneous structures. J Manuf Syst. 1997;16:239–48.
51. Sujith R, Jothi S, Zimmermann A, Aldinger F, Kumar R. Mechanical behaviour of polymer derived ceramics—a review. Int Mater Rev. 2021;66:426–49. https://doi.org/10.1080/09506608.2020.1784616
52. Pennstate: $4.5M grant to fund 3D-printed high-performance ceramics project, https://www.matse.psu.edu/article/45m-grant-fund-3d-printed-high-performance-ceramics-project
53. King WE, Anderson AT, Ferencz RM, Hodge NE, Kamath C, Khairallah SA, et al: Laser powder bed fusion additive manufacturing of metals; physics, computational, and materials challenges. Appl Phys Rev. 2015;2:041304. https://doi.org/10.1063/1.4937809
54. Sing SL, Yeong WY. Laser powder bed fusion for metal additive manufacturing: perspectives on recent developments. Virtual Phys Prototyp. 2020;15:359–70. https://doi.org/10.1080/17452759.2020.1779999
55. Gibson I, Rosen D, Stucker B. Additive manufacturing technologies: 3D printing, rapid prototyping, and direct digital manufacturing, second edition. New York: Springer; 2015.
56. Papazoglou EL, Karkalos NE, Karmiris-Obratański P, Markopoulos AP. On the modeling and simulation of SLM and SLS for metal and polymer powders: a review. Arch Comput Meth Eng. 2022;29:941–73. https://doi.org/10.1007/s11831-021-09601-x
57. Fatemeh Nabavi S, Farshidianfar A, Dalir H. Comprehensive review: advancements in modeling geometrical and mechanical characteristics of laser powder bed fusion process. Opt Laser Technol. 2025;180:111480. https://doi.org/10.1016/j.optlastec.2024.111480
58. Ge Y, Yang A, Chang Z, Ma N, Wang Q. Enhancing reliability in laser powder bed fusion through substrate modification: microstructure, mechanical properties and residual stress. Opt Laser Technol. 2025;181:111612. https://doi.org/10.1016/j.optlastec.2024.111612
59. Nouri A, Rohani Shirvan A, Li Y, Wen C. Additive manufacturing of metallic and polymeric load-bearing biomaterials using laser powder bed fusion: a review. J Mater Sci Technol. 2021;94:196–215. https://doi.org/10.1016/j.jmst.2021.03.058
60. Khosravani MR, Frohn-Sörensen P, Engel B, Reinicke T. Improvement of strength in single-lap adhesive joints of AlSi10Mg alloys fabricated by laser powder bed fusion. Eur J Mech A-Solid. 2025;109:105458. https://doi.org/10.1016/j.euromechsol.2024.105458
61. Luo X, Yang C, Li D, Zhang L-C. Laser powder bed fusion of beta-type titanium alloys for biomedical application: a review. Acta Metallurgica Sinica (English Letters). 2024;37:17–28. https://doi.org/10.1007/s40195-023-01654-0
62. Sun C, Zhang S, Tu R, Wu L, Ye J, Shi Y, et al: Additive manufacturing of gradient porous Si/SiC ceramic parts: quasi-static behaviors and mechanical properties. Compos Struct. 2025;352:118693. https://doi.org/10.1016/j.compstruct.2024.118693
63. Wang Y, Wu T, Huang G. State-of-the-art research progress and challenge of the printing techniques, potential applications for advanced ceramic materials 3D printing. Mater Today Commun. 2024;40:110001. https://doi.org/10.1016/j.mtcomm.2024.110001
64. Zhang Y, Xiong Z, Zhang K, Liao W, Liu T, Kuang W, et al: Microstructural and mechanical analysis of (Y0.2Yb0.2Lu0.2Eu0.2Er0.2)3Al5O12 high-entropy oxide ceramic fabricated in-situ via laser powder bed fusion. J Eur Ceram Soc. 2025;45:117072. https://doi.org/10.1016/j.jeurceramsoc.2024.117072
65. Liu Y, Zhang Y, Guo Z, Lu W. Effect of laser power, speed and offset on the welding performance of 304 SS/Al2O3 ceramics. Ceram Int. 2024;50:5384–401. https://doi.org/10.1016/j.ceramint.2023.11.289
66. Zhang K, Li S, Liu T, Xiong Z, Zhu Z, Zhang Y, et al: Broadening the microstructure regime of Al2O3–ZrO2 hypereutectic ceramic fabricated via laser powder bed fusion. Smart Mater Res. 2024;2:100048. https://doi.org/10.1016/j.smmf.2024.100048
67. Zhang J, Wu J-M, Liu H, Zheng W, Ye C-S, Wen S-F, et al: Microstructure and properties of silica-based ceramic cores by laser powder bed fusion combined with vacuum infiltration. J Mater Sci Technol. 2023;157:71–79. https://doi.org/10.1016/j.jmst.2022.12.078
68. Liu H, Zhang R-Z, Wu J-M, Li W-K, Zhou S-X, Zhang J, et al: Effect of Al(OH)3 on the properties of silica-based ceramic cores prepared by laser powder bed fusion combined with vacuum infiltration. Addit Manuf. 2024;95:104527. https://doi.org/10.1016/j.addma.2024.104527
69. Xi S, Chen H, Zhou J, Zheng L, Wang W, Zheng Q. Microstructure evolution and wear resistance of a novel ceramic particle-reinforced high-entropy alloy prepared by laser powder bed fusion. Ceram Int. 2024;50:5962–73. https://doi.org/10.1016/j.ceramint.2023.11.162
70. Maurya HS, Kollo L, Juhani K, Sergejev F, Prashanth KG. Effect of preheating and cooling of the powder bed by laser pulse shaping on the microstructure of the TiC based cermets. Ceram Int. 2022;48:20612–18. https://doi.org/10.1016/j.ceramint.2022.04.029
71. Zheng Y, Zhang K, Liu TT, Liao WH, Zhang CD, Shao H. Cracks of alumina ceramics by selective laser melting. Ceram Int. 2019;45:175–84. https://doi.org/10.1016/j.ceramint.2018.09.149
72. Verga F, Borlaf M, Conti L, Florio K, Vetterli M, Graule T, et al: Laser-based powder bed fusion of alumina toughened zirconia. Addit Manuf. 2020;31:100959. https://doi.org/10.1016/j.addma.2019.100959
73. Shen Z, Su H, Yu M, Guo Y, Liu Y, Zhao D, et al: Large-size complex-structure ternary eutectic ceramic fabricated using laser powder bed fusion assisted with finite element analysis. Addit Manuf. 2023;72:103627. https://doi.org/10.1016/j.addma.2023.103627
74. Montón Zarazaga A, Abdelmoula M, Küçüktürk G, Maury F, Ferrato M, Grossin D. Process parameters investigation for direct powder bed selective laser processing of silicon carbide parts. Progress in Additive Manufacturing. 2022;7:1307–22. https://doi.org/10.1007/s40964-022-00305-7
75. Juste E, Petit F, Lardot V, Cambier F. Shaping of ceramic parts by selective laser melting of powder bed. J Mater Res. 2014;29:2086–94. https://doi.org/10.1557/jmr.2014.127
76. Mazur M, Selvakannan PR. Laser powder bed fusion—principles, challenges, and opportunities. In: Bhargava SK,

Ramakrishna S, Brandt M, Selvakannan PR (eds.) Additive manufacturing for chemical sciences and engineering. Singapore: Springer Nature Singapore; 2022. p. 77–108.
77. Joe DJ, Kim S, Park JH, Park DY, Lee HE, Im TH, et al: Laser–material interactions for flexible applications. Adv Mater. 2017;29:1606586. https://doi.org/10.1002/adma.201606586
78. Simonds BJ, Tanner J, Artusio-Glimpse A, Williams PA, Parab N, Zhao C, et al: The causal relationship between melt pool geometry and energy absorption measured in real time during laser-based manufacturing. Appl Mater Today. 2021;23:101049. https://doi.org/10.1016/j.apmt.2021.101049
79. Pinkerton AJ. [INVITED] Lasers in additive manufacturing. Opt Laser Technol. 2016;78:25–32. https://doi.org/10.1016/j.optlastec.2015.09.025
80. Bayat M, Rothfelder R, Schwarzkopf K, Zinoviev A, Zinovieva O, Spurk C, et al: Exploring spatial beam shaping in laser powder bed fusion: high-fidelity simulation and in-situ monitoring. Addit Manuf. 2024;93:104420. https://doi.org/10.1016/j.addma.2024.104420
81. Wischeropp TM. Effect of laser beam profile on SLM process. In: Advancement of selective laser melting by laser beam shaping. Berlin, Heidelberg: Springer Berlin Heidelberg; 2021. p. 61–112.
82. Hung C-H, Chu C-W, Chang T-L, Lin T-C, Chen Y-P. Effect of focal spot size on AlSi10Mg alloy parts fabricated by laser powder bed fusion: process window, mechanical properties, and microstructure. J Alloys Compd. 2024;977:173338. https://doi.org/10.1016/j.jallcom.2023.173338
83. Cozzolino E, Tiley AJ, Ramirez AJ, Astarita A, Herderick ED. Energy efficiency of Gaussian and ring profiles for LPBF of nickel alloy 718. Int J Adv Manuf Tech. 2024;132:3093–104. https://doi.org/10.1007/s00170-024-13511-0
84. Xiong Z, Zhang K, Liu T, Zhu Z, Wei H, Zou Z, et al: Role of scanning speed on the microstructure and mechanical properties of additively manufactured Al2O3–ZrO2. J Am Ceram Soc. 2023;106:7760–75. https://doi.org/10.1111/jace.19385
85. Panwisawas C, Tang YT, Reed RC. Metal 3D printing as a disruptive technology for superalloys. Nat Commun. 2020;11:2327. https://doi.org/10.1038/s41467-020-16188-7
86. Liu Z, Ma C, Chang Z, Yan P, Li F. Advances in crack formation mechanism and inhibition strategy for ceramic additive manufacturing. J Eur Ceram Soc. 2023;43:5078–98. https://doi.org/10.1016/j.jeurceramsoc.2023.05.008
87. Liu L, Wang D, Yang Y, Wang Z, Qian Z, Wu S, et al: Effect of scanning strategies on the microstructure and mechanical properties of inconel 718 alloy fabricated by laser powder bed fusion. Adv Eng Mater. 2023;25:2200492. https://doi.org/10.1002/adem.202200492
88. Vikram RJ, Gokulnath SA, Prashanth KG, Suwas S. Effect of scanning strategy on microstructure and texture evolution in a selective laser melted Al-33Cu eutectic alloy. J Alloys Compd. 2023;936:168098. https://doi.org/10.1016/j.jallcom.2022.168098
89. Ali H, Ghadbeigi H, Mumtaz K. Effect of scanning strategies on residual stress and mechanical properties of Selective Laser Melted Ti6Al4V. Mater Sci Eng A. 2018;712:175–87. https://doi.org/10.1016/j.msea.2017.11.103
90. Ullah A, Wu H, Ur Rehman A, Zhu Y, Liu T, Zhang K. Influence of laser parameters and Ti content on the surface morphology of L-PBF fabricated Titania. Rapid Prototyp J. 2021;27:71–80. https://doi.org/10.1108/RPJ-03-2020-0050
91. Zhang Y, Zhang K, Chen D, Liu T, Xiong Z, Li S, et al: Morphology and formation mechanism of cracks in Al2O3–ZrO2 eutectic ceramics fabricated via laser powder bed fusion. J Am Ceram Soc. 2024;107:2128–42. https://doi.org/10.1111/jace.19586
92. Fedina T. Laser beam-material interaction in Powder Bed Fusion.
93. Belay GY, Kinds Y, Goossens L, Gurung K, Bosmans N, Diltoer R, et al: Dynamic optical beam shaping system to generate Gaussian and top-hat laser beams of various sizes with circular and square footprint for Additive Manufacturing applications. Procedia CIRP. 2022;111:75–80. https://doi.org/10.1016/j.procir.2022.08.134
94. Feuchtenbeiner S, Dubitzky W, Hesse T, Speker N, Haug P, Seebach J, et al: Beam shaping BrightLine Weld: latest application results. In: Kaierle S, Heinemann SW (eds.) High-power laser materials processing: applications, diagnostics, and systems VIII. SPIE; 2019. p. 109110X.
95. Almeida J, Liang D, Vistas CR. A doughnut-shaped Nd:YAG solar laser beam. Opt Laser Technol. 2018;106:1–6. https://doi.org/10.1016/j.optlastec.2018.03.029
96. Paillier G, Prätzsch N. Beam shaping to tackle laser powder bed fusion challenges. PhotonicsViews. 2024;21:30–35. https://doi.org/10.1002/phvs.202400021
97. Moore R, Orlandi G, Rodgers T, Moser D, Murdoch H, Abdeljawad F. Microstructure-based modeling of laser beam shaping during additive manufacturing. JOM. 2024;76:1726–36. https://doi.org/10.1007/s11837-023-06363-8
98. Bauch A, Kohlwes P, Kelbassa I. Laser powder bed fusion of pure copper using ring-shaped beam profiles. J Laser Appl. 2024;36:042021. https://doi.org/10.2351/7.0001562
99. Schwarzkopf K, Burger S, Chechik L, Forster C, Döring M, Spurk C, et al: Revealing the influence of ring-shaped beam profiles in high-speed laser beam microwelding by synchrotron x-ray imaging. J Laser Appl. 2024;36:042027. https://doi.org/10.2351/7.0001582
100. Chechik L, Schwarzkopf K, Rothfelder R, Grünewald J, Schmidt M. Material dependent influence of ring/spot beam profiles in laser powder bed fusion. Additive Manufacturing Letters. 2024;9:100211. https://doi.org/10.1016/j.addlet.2024.100211
101. R Martinsen A Rudolf D Kliner: Ring beams change the game for powder-bed fusion. https://www.laserfocusworld.com/laser-processing/article/14280827/ring-beams-change-the-game-for-powder-bed-fusion
102. Nguejio J, Mokhtari M, Paccou E, Baustert E, Khalij L, Hug E, et al: Combined effect of a spread powder particle size distribution, surface machining and stress-relief heat treatment on microstructure, tensile and fatigue properties of 316L steel manufactured by laser powder bed fusion. Int J Adv Manuf Tech. 2024;131:563–83. https://doi.org/10.1007/s00170-023-11008-w
103. Chu F, Shen H, Liu J, Hou J, Zhang K, Zhou Z, et al: Improved ductility by reducing powder size in laser powder bed fusion of AlSi10Mg. Additive Manufacturing Frontiers. 2024;3:200122. https://doi.org/10.1016/j.amf.2024.200122
104. Chu F, Li E, Shen H, Chen Z, Li Y, Liu H, et al: Influence of powder size on defect generation in laser powder bed fusion

of AlSi10Mg alloy. J Manuf Process. 2023;94:183–95. https://doi.org/10.1016/j.jmapro.2023.03.046

105. Zhao Y, He J, Li B, Gao Z, Guo Q, Ma Z, et al: The role of ceramic particles on the crack inhibition and mechanical properties improvement of Haynes 230 alloy fabricated by laser powder bed fusion. J Mater Process Technol. 2023;320:118124. https://doi.org/10.1016/j.jmatprotec.2023.118124
106. Karabulut Y, Ünal R. Additive manufacturing of ceramic particle-reinforced aluminum-based metal matrix composites: a review. J Mater Sci. 2022;57:19212–42. https://doi.org/10.1007/s10853-022-07850-0
107. Maurya HS, Kosiba K, Juhani K, Sergejev F, Prashanth KG. Effect of powder bed preheating on the crack formation and microstructure in ceramic matrix composites fabricated by laser powder-bed fusion process. Addit Manuf. 2022;58:103013. https://doi.org/10.1016/j.addma.2022.103013
108. Sun M, Yang Z, Zhang J, Zhang S, Yang Q, Song S, et al: Effects of ZrO2 nanoparticles on the microstructure and mechanical properties of ZrO2/AlSi10Mg composites manufactured by laser powder bed fusion. Ceram Int. 2023;49:19673–81. https://doi.org/10.1016/j.ceramint.2023.03.080
109. Sofia D, Barletta D, Poletto M. Laser sintering process of ceramic powders: the effect of particle size on the mechanical properties of sintered layers. Addit Manuf. 2018;23:215–24. https://doi.org/10.1016/j.addma.2018.08.012
110. Shanthar R, Chen K, Abeykoon C. Powder-based additive manufacturing: a critical review of materials, methods, opportunities, and challenges. Adv Eng Mater. 2023;25:2300375. https://doi.org/10.1002/adem.202300375
111. Xing M, Wang H, Zhao Z, Zhang Y, Lou H, Liu C, et al: SLM printing of cermet powders: inhomogeneity from atomic scale to microstructure. Ceram Int. 2022;48:29892–99. https://doi.org/10.1016/j.ceramint.2022.06.254
112. Zhang M, Fang B, Fan L. Optimizing powder morphology and scanning strategies to enhance shape accuracy in L-PBF alumina ceramic formation. Ceram Int. (2024). https://doi.org/10.1016/j.ceramint.2024.12.240
113. Deirmina F, Adegoke O, Col MD, Pellizzari M. Effect of layer thickness, and laser energy density on the recrystallization behavior of additively manufactured Hastelloy X by laser powder bed fusion. Additive Manufacturing Letters. 2023;7:100182. https://doi.org/10.1016/j.addlet.2023.100182
114. Hyer HC, Petrie CM. Effect of powder layer thickness on the microstructural development of additively manufactured SS316. J Manuf Process. 2022;76:666–74. https://doi.org/10.1016/j.jmapro.2022.02.047
115. Liu S, Shin YC. Additive manufacturing of Ti6Al4V alloy: a review. Mater Des. 2019;164:107552. https://doi.org/10.1016/j.matdes.2018.107552
116. Elkholy A, Narvan M, Thompson S, Durfee J, Kempers R. The effect of layer thickness on the geometry and capillary performance of strut-based heat pipe wicks manufactured by laser powder bed fusion. Int J Therm. 2024;21:100543. https://doi.org/10.1016/j.ijft.2023.100543
117. Rońda N, Grzelak K, Polański M, Dworecka-Wójcik J. The influence of layer thickness on the microstructure and mechanical properties of m300 maraging steel additively manufactured by LENS® technology. Materials. 2022;15:603. https://doi.org/10.3390/ma15020603
118. Xiong Z, Zhang K, Zhu Z, Liu T, Zhang Y, Li S, et al: Effect of laser focus shift on the forming quality, microstructure and mechanical properties of additively manufactured Al2O3–ZrO2 eutectic ceramics. Ceram Int. 2023;49:35948–62. https://doi.org/10.1016/j.ceramint.2023.08.275
119. Fang B, Cheng C, Zhang M, Fan L. Effect of forming strategy on surface morphology and properties of zirconia ceramics formed by laser powder bed fusion. Ceram Int. 2024;50:13176–84. https://doi.org/10.1016/j.ceramint.2024.01.229
120. Ullah A, Asami K, Azher K, Emmelmann C. Comparative analysis of laser power, pure titanium, and titanium alloy effects on dendrite growth and surface morphology of TiO2-ceramic. J Laser Appl. 2024;36:042061. https://doi.org/10.2351/7.0001601
121. Wilson-Heid AE, Griffiths RJ, Martin AA, Holliday KS, Jeffries JR. Exploring laser-material interactions of zirconium carbide under additive manufacturing conditions. Ceram Int. 2024;50:23275–83. https://doi.org/10.1016/j.ceramint.2024.04.051
122. Peters AB, Zhang D, Hernandez A, Wang C, Nagle DC, Mueller T, et al: Selective laser reaction synthesis of SiC, Si3N4 and HfC/SiC composites for additive manufacturing. J Eur Ceram Soc. 2023;43:1270–83. https://doi.org/10.1016/j.jeurceramsoc.2022.11.015
123. Liu H, Jiang H, Chen Q, Shen Z, Zhang X, Liu H, et al: Insights into the applicability of laser energy density in directly preparing Al2O3-based eutectic ceramics by laser additive manufacturing. Ceram Int. 2024;50:3381–87. https://doi.org/10.1016/j.ceramint.2023.11.084
124. Abdelmoula M, Küçüktürk G, Juste E, Petit F. Enhancing powder bed fusion of alumina ceramic material: a comprehensive study from powder tailoring to mechanical performance evaluation. Int J Adv Manuf Tech. 2024;131:1745–67. https://doi.org/10.1007/s00170-024-13158-x
125. Gu D, Hagedorn Y-C, Meiners W, Meng G, Batista RJS, Wissenbach K, et al: Densification behavior, microstructure evolution, and wear performance of selective laser melting processed commercially pure titanium. Acta Mater. 2012;60:3849–60. https://doi.org/10.1016/j.actamat.2012.04.006
126. Haribaskar R, Kumar TS. Defects in metal additive manufacturing: formation, process parameters, postprocessing, challenges, economic aspects, and future research directions. 3D Print Addit Manuf. 11, e1629–55 (2024). https://doi.org/10.1089/3dp.2022.0344
127. Gong H, Rafi H, Gu H, Ram G, Starr T, Stucker B. Influence of defects on mechanical properties of Ti-6Al-4V components produced by selective laser melting and electron beam melting. Mater Des. 86, (2015). https://doi.org/10.1016/j.matdes.2015.07.147
128. Ullah A, Ur Rehman A, Salamci MU, Ptr F, Liu T. The influence of laser power and scanning speed on the microstructure and surface morphology of Cu2O parts in SLM. Rapid Prototyp J. 2022;28:1796–807. https://doi.org/10.1108/RPJ-12-2021-0342
129. Shen Z, Su H, Yu M, Guo Y, Liu Y, Jiang H, et al: Enhanced 3D printing and crack control in melt-grown eutectic ceramic composites with high-entropy alloy doping. J Mater Sci Technol. 2025;209:64–78. https://doi.org/10.1016/j.jmst.2024.04.076
130. Tavangarian F, Hui D, Li G. Crack-healing in ceramics. Compos B Eng. 2018;144:56–87. https://doi.org/10.1016/j.compositesb.2018.02.025

131. Punj S, Singh J, Singh K. Ceramic biomaterials: Properties, state of the art and future prospectives. Ceram Int. 2021;47:28059–74. https://doi.org/10.1016/j.ceramint.2021.06.238
132. Blatz MB, Sadan A, Kern M. Resin-ceramic bonding: a review of the literature. J Prosthet Dent. 2003;89:268–74. https://doi.org/10.1067/mpr.2003.50
133. Huang Y, Wu D, Li C, Lv W, Ma G, Zhou C, Niu F. Investigation on the cracking mechanism of melt growth alumina/aluminum titanate ceramics prepared by laser directed energy deposition. Chinese Journal of Mechanical Engineering: Additive Manufacturing Frontiers. 2023;2:100099. https://doi.org/10.1016/j.cjmeam.2023.100099
134. Huang Y, Wu D, Yu X, Ma G, Han J, Wang H, et al: Cracking mechanism in laser directed energy deposition of melt growth alumina/aluminum titanate ceramics. J Am Ceram Soc. 2023;106:4358–70. https://doi.org/10.1111/jace.19080
135. Wu D, San J, Niu F, Zhao D, Liang X, Yan S, et al: Effect and mechanism of ZrO2 doping on the cracking behavior of melt-grown Al2O3 ceramics prepared by directed laser deposition. Int J Appl Ceram Technol. 2020;17:227–38. https://doi.org/10.1111/ijac.13374
136. Abolhasani D, Hossein Seyedkashi SM, Hwang TW, Moon YH. Selective laser melting of AISI 304 stainless steel composites reinforced by Al2O3 and eutectic mixture of Al2O3–ZrO2 powders. Materials Science and Engineering: A. 2019;763:138161. https://doi.org/10.1016/j.msea.2019.138161
137. Sharma SK, Grewal HS, Saxena KK, Mohammed KA, Prakash C, Davim JP, et al: Advancements in the additive manufacturing of magnesium and aluminum alloys through laser-based approach. Materials. 2022;15:8122. https://doi.org/10.3390/ma15228122
138. Ur Rehman A, Saleem MA, Liu T, Zhang K, Pitir F, Salamci MU. Influence of silicon carbide on direct powder bed selective laser process (sintering/melting) of alumina. Materials. 15, (2022). https://doi.org/10.3390/ma15020637
139. Liu Q, Danlos Y, Song B, Zhang B, Yin S, Liao H. Effect of high-temperature preheating on the selective laser melting of yttria-stabilized zirconia ceramic. J Mater Process Technol. 222, (2015). https://doi.org/10.1016/j.jmatprotec.2015.02.036
140. Wilkes J, Hagedorn Y-C, Meiners W, Wissenbach K. Additive manufacturing of ZrO2-Al2O3 ceramic components by selective laser melting. Rapid Prototyp J. 19, (2013). https://doi.org/10.1108/13552541311292736
141. Maurya HS, Kollo L, Tarraste M, Juhani K, Sergejev F, Prashanth KG. Selective laser melting of TiC-based cermet: HIP studies. Trans Indian Inst Met. 2023;76:565–70. https://doi.org/10.1007/s12666-022-02684-5
142. Zhou Y, Dong X, Li N, Yan J. Effects of post-treatment on metal-ceramic bond properties of selective laser melted Co-Cr dental alloy. Part 1: annealing temperature. J Prosthet Dent. 2023;129:657.e1–657.e9. https://doi.org/10.1016/j.prosdent.2022.11.029
143. Ur Rehman A, Ullah A, Liu T, Ur Rehman R, Salamci MU, Liao W. Selective laser oxidation sintering of cuprous oxide. Materials Letters: X. 2023;17:100172. https://doi.org/10.1016/j.mlblux.2022.100172
144. Pfeiffer S, Florio K, Makowska M, Aneziris CG, Van Swygenhoven H, Wegener K, et al: Crack-reduced laser powder bed fused oxide ceramic parts by in-situ synthesis of negative thermal expansion phases. J Eur Ceram Soc. 2024;44:1012–26. https://doi.org/10.1016/j.jeurceramsoc.2023.09.040
145. Kaya D, Abdelmoula M, Küçüktürk G, Grossin D, Stamboulis A. A novel approach for powder bed fusion of ceramics using two laser systems. Materials. 2023;16:2507. https://doi.org/10.3390/ma16062507
146. Wu S, Sha G, Yang L, Wang C, Duan Q, Yan C, et al: Mechanical characteristics of Si/SiC graded ceramic lattice structures with a triply periodic minimal surface fabricated by laser powder bed fusion. Compos Struct. 2024;346:118417. https://doi.org/10.1016/j.compstruct.2024.118417
147. Özmen E, Grossin D, Lenormand P, Bertrand G. Direct powder bed selective laser processing of dense alumina-toughened zirconia parts. Progress in Additive Manufacturing. 2024. https://doi.org/10.1007/s40964-024-00755-1
148. Wu S, Yang L, Yan C, Shi Y. Fatigue properties of SiC graded ceramic lattice structures with a triply periodic minimal surface manufactured by laser powder bed fusion. J Eur Ceram Soc. 2024;44:116695. https://doi.org/10.1016/j.jeurceramsoc.2024.116695
149. Grossin D, Montón A, Navarrete-Segado P, Özmen E, Urruth G, Maury F, et al: A review of additive manufacturing of ceramics by powder bed selective laser processing (sintering /melting): calcium phosphate, silicon carbide, zirconia, alumina, and their composites. Open Ceramics. 2021;5:100073. https://doi.org/10.1016/j.oceram.2021.100073
150. Dong Y, Chen A, Yang T, Gao S, Liu S, Guo B, et al: Microstructure evolution and mechanical properties of Al2O3 foams via laser powder bed fusion from Al particles. Adv Powder Mater. 2023;2:100135. https://doi.org/10.1016/j.apmate.2023.100135
151. Wang R, Qiao G, Song G. Additive manufacturing by laser powder bed fusion and thermal post-treatment of the lunar-regolith-based glass-ceramics for in-situ resource utilization. Constr Build Mater. 2023;392:132051. https://doi.org/10.1016/j.conbuildmat.2023.132051
152. Wang D, Han H, Sa B, Li K, Yan J, Zhang J, et al: A review and a statistical analysis of porosity in metals additively manufactured by laser powder bed fusion. Opto-Electronic Advances. 2020;5:210058. https://doi.org/10.29026/oea.2022.210058
153. Sinha S, Mukherjee T. Mitigation of gas porosity in additive manufacturing using experimental data analysis and mechanistic modeling. Materials. 2024;17:1569. https://doi.org/10.3390/ma17071569
154. Liu Z, Ma C, Chang Z, Zhao P, Zhang Y, Wu Q, et al: Formation mechanism and quantitative analysis of pores in Al2O3–ZrO2 ceramic different structures by laser additive manufacturing. Ceram Int. 2023;49:16099–109. https://doi.org/10.1016/j.ceramint.2023.01.208
155. Marattukalam JJ, Pacheco V, Karlsson D, Riekehr L, Lindwall J, Forsberg F, et al: Development of process parameters for selective laser melting of a Zr-based bulk metallic glass. Addit Manuf. 2020;33:101124. https://doi.org/10.1016/j.addma.2020.101124
156. Lei J, Zhang Q, Wang Y, Zhang H. Direct laser melting of Al2O3 ceramic paste for application in ceramic additive manufacturing. Ceram Int. 2022;48:14273–80. https://doi.org/10.1016/j.ceramint.2022.01.315
157. Yao L, Xiao Z, Huang S, Ramamurty U. The formation mechanism of metal-ceramic interlayer interface during laser powder

bed fusion. Virtual Phys Prototyp. 18, e2235324 (2023). https://doi.org/10.1080/17452759.2023.2235324

158. Rehman AU, Ullah A, Liu T, Rehman RU, Salamci MU. Additive manufacturing of Al2O3 ceramics with MgO/SiC contents by laser powder bed fusion process. Front Chem. 11, (2023). https://doi.org/10.3389/fchem.2023.1034473
159. Azami M, Siahsarani A, Hadian A, Kazemi Z, Rahmatabadi D, Kashani-Bozorg SF, et al: Laser powder bed fusion of alumina/Fe–Ni ceramic matrix particulate composites impregnated with a polymeric resin. J Mater Res Technol. 2023;24:3133–44. https://doi.org/10.1016/j.jmrt.2023.03.181
160. Zhou Y, Dong X, Li N, Yan J. Effects of post-treatment on metal-ceramic bond properties of selective laser melted Co-Cr dental alloy. Part 1: Annealing temperature. J Prosthet Dent. 129, 657.e1–657.e9 (2023). https://doi.org/10.1016/j.prosdent.2022.11.029
161. Sripada J, Tian Y, Chadha K, Saha G, Jahazi M, Spray J, et al: Effect of hot isostatic pressing on microstructural and micromechanical properties of additively manufactured 17–4PH steel. Mater Charact. 2022;192:112174. https://doi.org/10.1016/j.matchar.2022.112174
162. Ng CH, Bermingham MJ, Dargusch MS. Eliminating porosity defects, promoting equiaxed grains and improving the mechanical properties of additively manufactured Ti-22V-4Al with super-transus hot isostatic pressing. Addit Manuf. 2023;72:103630. https://doi.org/10.1016/j.addma.2023.103630
163. Rehman AU, Mahmood MA, Ansari P, Pitir F, Salamci MU, Popescu AC, et al: Spatter formation and splashing induced defects in laser-based powder bed fusion of AlSi10Mg alloy: a novel hydrodynamics modelling with empirical testing. Metals (Basel). 11, (2021). https://doi.org/10.3390/met11122023
164. Wischeropp T. Advancement of selective laser melting by laser beam shaping. 2021.
165. Bakhtari AR, Sezer HK, Canyurt OE, Eren O, Shah M, Marimuthu S. A review on laser beam shaping application in laser-powder bed fusion. Adv Eng Mater. 2024;26:2302013. https://doi.org/10.1002/adem.202302013
166. Wu Y-R, He J-H, Cheng L-J, Wu J-M, Shi Y-S. Effects of AlN inorganic binder on the properties of porous Si3N4 ceramics prepared by selective laser sintering. Ceram Int. 2022;48:29900–29906. https://doi.org/10.1016/j.ceramint.2022.06.255
167. Liu S-S, Li M, Wu J-M, Chen A-N, Shi Y-S, Li C-H. Preparation of high-porosity Al2O3 ceramic foams via selective laser sintering of Al2O3 poly-hollow microspheres. Ceram Int. 2020;46:4240–47. https://doi.org/10.1016/j.ceramint.2019.10.144
168. Zhang H, LeBlanc S. Processing parameters for selective laser sintering or melting of oxide ceramics. In: Shishkovsky, IV (ed.) Additive manufacturing of high-performance metals and alloys. Rijeka: IntechOpen; 2018. p. Ch. 5
169. Simson D, Subbu SK. Effect of process parameters on surface integrity of LPBF Ti6Al4V. Procedia CIRP. 2022;108:716–21. https://doi.org/10.1016/j.procir.2022.03.111
170. Ullah A, Wu H, Rehman AU, Zhu Y, Liu T, Zhang K. Influence of laser parameters and Ti content on the surface morphology of L-PBF fabricated Titania. Rapid Prototyp J. 2021;27:71–80. https://doi.org/10.1108/RPJ-03-2020-0050
171. Simson D, Paul CP, Subbu SK. Experimental study and neural network model based prediction of layer thickness influence on LPBF IN625 single track geometry. Opt Laser Technol. 2024;173:110543. https://doi.org/10.1016/j.optlastec.2024.110543
172. Travitzky N, Bonet A, Dermeik B, Fey T, Filbert-Demut I, Schlier L, et al: Additive manufacturing of ceramic-based materials. Adv Eng Mater. 2014;16:729–54. https://doi.org/10.1002/adem.201400097
173. Pelevin IA, Nalivaiko AY, Ozherelkov DY, Shinkaryov AS, Chernyshikhin SV, Arnautov AN, et al: Selective laser melting of al-based matrix composites with Al2O3 reinforcement: features and advantages. Materials. 2021;14:2648. https://doi.org/10.3390/ma14102648
174. Gao B, Zhao H, Peng L, Sun Z. A review of research progress in selective laser melting (SLM). Micromachines (Basel). 2023;14:57. https://doi.org/10.3390/mi14010057
175. Han Q, Setchi R, Lacan F, Gu D, Evans SL. Selective laser melting of advanced Al-Al2O3 nanocomposites: simulation, microstructure and mechanical properties. Mater Sci Eng A. 2017;698:162–73. https://doi.org/10.1016/j.msea.2017.05.061
176. Jue J, Gu D, Chang K, Dai D. Microstructure evolution and mechanical properties of Al-Al2O3 composites fabricated by selective laser melting. Powder Technol. 2017;310:80–91. https://doi.org/10.1016/j.powtec.2016.12.079
177. Xiong Z, Zhang K, Liao W, Liu T, Liu X, Zhu Z. Laser powder bed fusion fabrication of TiB2-modified Al2O3-ZrO2 eutectic ceramics: microstructure evolution and mechanical properties. Ceram Int. 2024;50:55577–88. https://doi.org/10.1016/j.ceramint.2024.10.418
178. Jue J, Gu D. Selective laser melting additive manufacturing of in situ Al2Si4O10/Al composites: microstructural characteristics and mechanical properties. J Compos Mater. 2017;51:519–32. https://doi.org/10.1177/0021998316649251
179. Shen Z, Su H, Liu H, Zhao D, Liu Y, Guo Y, et al: Directly fabricated Al2O3/GdAlO3 eutectic ceramic with large smooth surface by selective laser melting: rapid solidification behavior and thermal field simulation. J Eur Ceram Soc. 2022;42:1088–101. https://doi.org/10.1016/j.jeurceramsoc.2021.11.003
180. Li S, Zhang K, Yan Z, Liu T, Zhu Z, Xiong Z, et al: Effect of Nb addition on the microstructure and mechanical properties of additively manufactured Ti2AlC MAX-phase ceramic matrix composites. Addit Manuf. 2023;67:103488. https://doi.org/10.1016/j.addma.2023.103488
181. Han Q, Setchi R, Lacan F, Gu D, Evans SL. Selective laser melting of advanced Al-Al2O3 nanocomposites: simulation, microstructure and mechanical properties. Materials Science and Engineering: A. 2017;698:162–73. https://doi.org/10.1016/j.msea.2017.05.061
182. Shen Z, Su H, Yu M, Guo Y, Liu Y, Zhao D, et al: Large-size complex-structure ternary eutectic ceramic fabricated using laser powder bed fusion assisted with finite element analysis. Additive Manufacturing. 72 (2023) 103627 Available online 25. 2214–8604 (2023). https://doi.org/10.1016/j.addma.2023.103627
183. Shuai C, Feng P, Gao C, Zhou Y, Peng S. Simulation of dynamic temperature field during selective laser sintering of ceramic powder. Math Comput Model Dyn Syst. 2013;19:1–11. https://doi.org/10.1080/13873954.2012.689769
184. Abdelmoula M, Küçüktürk G, Juste E, Petit F. Enhancing powder bed fusion of alumina ceramic material: a comprehensive study from powder tailoring to mechanical performance

evaluation. Int J Adv Manuf Technol. 2024;131:1745–67. https://doi.org/10.1007/S00170-024-13158-X/FIGURES/17
185. Chen Q, Guillemot G, Gandin CA, Bellet M. Three-dimensional finite element thermomechanical modeling of additive manufacturing by selective laser melting for ceramic materials. Addit Manuf. 2017;16:124–37. https://doi.org/10.1016/J.ADDMA.2017.02.005
186. Chen Q, Guillemot G, Gandin CA, Bellet M. Numerical modelling of the impact of energy distribution and Marangoni surface tension on track shape in selective laser melting of ceramic material. Addit Manuf. 2018;21:713–23. https://doi.org/10.1016/J.ADDMA.2018.03.003
187. Luo C, Qiu J, Yan Y, Yang J, Uher C, Tang X. Finite element analysis of temperature and stress fields during the selective laser melting process of thermoelectric SnTe. J Mater Process Technol. 2018;261:74–85. https://doi.org/10.1016/J.JMATPROTEC.2018.06.001
188. Moniz L, Chen Q, Guillemot G, Bellet M, Gandin CA, Colin C, et al: Additive manufacturing of an oxide ceramic by laser beam melting—comparison between finite element simulation and experimental results. J Mater Process Technol. 2019;270:106–17. https://doi.org/10.1016/J.JMATPROTEC.2019.02.004
189. Datsiou KC, Ashcroft I. Numerical investigation of laser powder bed fusion of glass. Glass Structures and Engineering. 2024;9:185–200. https://doi.org/10.1007/S40940-024-00257-0/FIGURES/14
190. Chowdhury S, Yadaiah N, Prakash C, Ramakrishna S, Dixit S, Gupta LR, et al: Laser powder bed fusion: a state-of-the-art review of the technology, materials, properties & defects, and numerical modelling. J Mater Res Technol. 2022;20:2109–72. https://doi.org/10.1016/J.JMRT.2022.07.121
191. Sun H, Lian Q, Shi Y, Wan L, Chen Y, Wu Y, et al: Numerical analysis of the effects of reinforcing particles on the residual stress of TiB2/Al-Si composites fabricated by laser powder bed fusion. J Mater Eng Perform. 2024;33:7465–78. https://doi.org/10.1007/S11665-024-09198-9/FIGURES/16
192. Roberts IA, Wang CJ, Esterlein R, Stanford M, Mynors DJ. A three-dimensional finite element analysis of the temperature field during laser melting of metal powders in additive layer manufacturing. Int J Mach Tools Manuf. 2009;49:916–23. https://doi.org/10.1016/J.IJMACHTOOLS.2009.07.004

How to cite this article: Ullah A, Shah M, Ali Z, Asami K, Ur Rehman A, Emmelmann C. Additive manufacturing of ceramics via the laser powder bed fusion process. Int J Appl Ceram Technol. 2025;e15087. https://doi.org/10.1111/ijac.15087